1996

# The Development, Molecular Characterization and Application of a Model Stratum Corneum Lipid System

Rita M. Hatfield

*Loyola University Chicago*

LOYOLA UNIVERSITY CHICAGO

# THE DEVELOPMENT, MOLECULAR CHARACTERIZATION AND APPLICATION OF A MODEL STRATUM CORNEUM LIPID SYSTEM

A DISSERTATION SUBMITTED TO

THE FACULTY OF THE GRADUATE SCHOOL

IN CANDIDACY FOR THE DEGREE OF

DOCTOR OF PHILOSOPHY

DEPARTMENT OF CHEMISTRY

BY

RITA M. HATFIELD

CHICAGO, IL

JANUARY 1996

ACKNOWLEDGMENTS

I would like to acknowledge my advisor, Professor Leslie W.-M. Fung, for her guidance in my graduate education and for her willingness to direct a project different from her own research interests. Dr. Fung's high standards and dedication to research have challenged me to strive for excellence in research.

In addition, I would like to thank Drs. Priscilla Walling from Helene Curtis Industries and Robert Harper from Hilltop Research for their initiation and support of this project.

I would also like to thank Helene Curtis Industries for giving me the opportunity to participate in this collaborative project. Their generous financial support for myself and for this project is greatly appreciated. Thanks also go to Loyola University for their willingness to participate in this project.

I also wish to acknowledge the many scientists at Helene Curtis who have provided me with technical assistance and for their helpful discussions, particularly Dr. Craig Herb.

In addition, I would also like to thank the many people who have worked in Dr. Fung's lab during my time there for their friendship and their willingness to share knowledge.

Special thanks go to my parents, my husband, and my brothers and sisters for their support and encouragement throughout my graduate career.

Finally, I wish to dedicate this dissertation to my mom and dad, John and Florence Mrowca, for emphasizing the importance of education throughout my life and to my husband, Greg, for encouraging me to achieve my professional and personal goals.

TABLE OF CONTENTS

IV. DISCUSSION

## LIST OF TABLES

Table

## LIST OF FIGURES

Figure

## LIST OF ABBREVIATIONS

| | |
|---|---|
| $2A_{max}$ | hyperfine splitting |
| 5-DSA | 5-doxylstearic acid |
| 12-DSA | 12-doxylstearic acid |
| $A_{700}$ | optical absorbance at 700 nm |
| ANTS | 1-aminonaphthalene-3,6,8-trisulfonic acid |
| DPPC | dipalmitoylphosphatidylcholine |
| DPX | p-xylylenebis(pyridinium)bromide |
| DSC | differential scanning calorimetry |
| EM | electron microscopy |
| EPR | electron paramagnetic resonance |
| $f_{AQUEOUS}$ | fraction of spin labels in the aqueous phase of LUVs |
| $f_{LIPID}$ | fraction of spin labels in the lipid phase of LUVs |
| $f_{LIPID}/f_{AQUEOUS}$ | partition ratio |
| $F_{max}$ | maximum fluorescence |
| HPTLC | high performance thin layer chromatography |
| LUVs | large unilamellar vesicles |
| MES | 2-[N-Morpholino]ethanesulfonic acid |
| MLVs | multilamellar vesicles |
| QELS | quasi elastic light scattering |

| | |
|---|---|
| PS | phosphatidylserine |
| SC | stratum corneum |
| SUVs | small unilamellar vesicles |

# CHAPTER I

# INTRODUCTION

## 1.1 Development of a Model Stratum Corneum (SC) Lipid System

The skin is a barrier for most substances entering or leaving the body, and yet selective permeability for certain molecules, including water molecules, is an essential function of skin (Scheuplein and Blank, 1971; Downing, 1992; Williams and Barry, 1992). The origin of the selective permeability of the skin, and its quantitative prediction in terms of the relevant physical and chemical properties of skin and of penetrating molecules, have been the focal point for the study of skin permeability (Scheuplein and Blank, 1971; Downing, 1992). The outermost layer of mammalian skin is the stratum corneum. The stratum corneum is composed of about 15 layers of dead cells (corneocytes) in a lipid matrix and consists of 5 to 15 % lipids (dry weight), 75 to 80 % proteins, and 5 to 10 % unknown materials (Williams and Barry, 1992). Despite their overall small percentage in the stratum corneum, lipids play an important role in the selective permeability of the skin. Removal of either the entire stratum corneum or just the lipid component of the stratum corneum in the skin resulted in similar increases in water flux through the modified skin (Blank, 1952; Onken and Moyer, 1963). In addition, the composition and structural arrangement of stratum corneum lipids affect topical drug delivery (Hadgraft et al., 1992). The lipid composition of the stratum corneum is unusual relative to many well-known biological membranes, consisting primarily of cholesterol, ceramides, free fatty acids and cholesterol sulfate, with little phospholipids

(Gray et al., 1982; Wertz et al., 1987). Although these lipids form lamellar sheets in intact stratum corneum (Elias and Friend, 1975; Madison et al., 1987), the stratum corneum membrane is believed to differ from the vast majority of mammalian cell membranes (Kitson et al., 1994). A better understanding of the molecular properties of stratum corneum lipids is critical to studies on the physiology and pathophysiology of the stratum corneum.

Many model systems have been prepared either for studies of the stratum corneum lipid properties or for studies of lipid - molecule interactions. These model systems include different dispersions of lipids in water or buffer solutions (Friberg and Osborne, 1985; White et al., 1988; Kittayanond et al., 1992; Kim et al., 1993a; Mattai et al., 1993; Kitson et al., 1994), sonicated lipid suspensions, including the preparation of small unilamellar vesicles (SUVs) (Gray and White, 1979; Wertz et al., 1986; Kittayonand et al., 1992; Blume et al., 1993; Kim et al., 1993b; Kitagawa et al., 1993), and large unilamellar vesicles (LUVs) prepared by extrusion methods (Abraham, 1992; Downing et al., 1993). We chose LUVs as the model system since LUVs were comparatively more stable than the often used but highly strained, meta-stable SUVs (Szoka, 1987). In addition, the LUV system can be characterized more quantitatively in terms of lipid concentration, surface area and volume than multilamellar vesicle (MLV) systems, which are also quite stable. Thus the LUV system, with known internal volume, lipid concentration, and surface curvature, could be used, for example, in detailed molecular studies of lipid-molecule interaction, or in quantitative determination of permeability and transport by stratum corneum lipids.

A variety of lipid compositions have been used in model systems. Although some use phospholipids as a model of the bilayer structure of the stratum corneum (Kitson et al., 1992),

most use different mixtures of ceramide, cholesterol, free fatty acid and cholesterol sulfate. Different ceramides, including epidermal ceramide (Gray and White, 1979; White et al., 1988; Abraham, 1992; Downing et al., 1993; Kim et al., 1993b) or bovine brain ceramide type III (Kittayanond et al., 1992; Blume et al., 1993; Kitson et al., 1994), type IV (Kitagawa et al., 1993), or a mixture of bovine brain type III and IV (Mattai et al., 1993), have been used. Various fatty acids, ranging from carnauba fatty acids (used to simulate C20 - C30 fatty acids, but not commercially available) (Abraham, 1992; Downing et al., 1993), to mixtures of fatty acids (Friberg and Osborne, 1985; Kim et al., 1993b; Mattai et al., 1993), to just palmitic acid (Wertz et al., 1986; Kittayanond et al., 1992; Blume et al., 1993; Kim et al., 1993a; Kitagawa et al., 1993; Kitson et al., 1994) have been used. Thus most of the model systems are qualitatively similar, but quantitatively very different. No systematic comparison of these model systems is available. In the first part of this dissertation, the development and molecular characterization of a model stratum corneum lipid LUV system is described. In the preparation of our LUVs, we used a lipid composition that was closer to that of the native system than that used in many of the above mentioned studies. We also used lipids that were conveniently (commercially) available.

## 1.2 Molecular Characterization of SC LUVs

In order to characterize our LUVs on the molecular level, we have used both cryo- and freeze-fracture electron microscopy (EM) to observe the shape of the vesicles, quasi elastic light scattering (QELS) to determine size distribution, differential scanning calorimetry (DSC) to obtain thermal transition temperature and spin label electron paramagnetic

resonance (EPR) techniques to monitor the molecular dynamics of lipids. Many of the physical techniques that we used have been extensively used in characterizing phospholipid vesicle systems. However, these techniques have not been applied to stratum corneum lipid systems until recently (Golden et al., 1987; Hou et al., 1991). Stability of the LUVs at different pH values was followed. We also demonstrate, by EPR techniques, how this model system can be used to study partitioning of molecules with slightly different structures (two different fatty acid derivative spin labels) resulting in very different partitioning in the stratum corneum lipid vesicles.

## 1.3 Application of SC LUVs to Study SC Lipid Interactions

In the second part of this dissertation, the SC LUV model lipid system described and characterized above is used to study the effects of altered lipid composition on lipid interactions.

In addition to its role in the barrier function of skin, the lipid composition of the stratum corneum can effect desquamation, i.e. the processes by which corneocytes at the skin surface detach from neighboring cells and are removed (Brysk and Rajaraman, 1992; Williams, 1992), leading to disorders of cornification or the processes involved in the production and maintenance of normal stratum corneum (Williams, 1992). Lipid abnormalities have been reported in both common scaling disorders like psoriasis and atopic dermatitis and inherited disorders like ichthyosis (Williams, 1992). We have incorporated the lipid modifications present in the diseased skin state, recessive x-linked ichthyosis, in our model LUV system. Recessive x-linked ichthyosis is clinically characterized by excessive

scaling of the skin due to prolonged stratum corneum retention (Elias et al., 1984) and biochemically characterized by a lack of the enzyme steroid sulfatase (Shapiro et al., 1978). Recessive x-linked ichthyosis is chosen for this study since its lipid modifications are known, with decreased cholesterol and increased cholesterol sulfate levels in the outer epidermal layers, the stratum granulosum and the stratum corneum (Williams and Elias, 1981; Elias et al., 1984). From analysis of human stratum corneum scale from several patients, Williams and Elias (1981) have reported 2.6 % (by weight) cholesterol sulfate and 15.6 % cholesterol in normal SC and 14.8 % cholesterol sulfate and 9 % cholesterol in recessive x-linked ichthyosis SC. The molecular mechanism by which cholesterol sulfate might prevent shedding of the stratum corneum is still unknown. Cholesterol sulfate is present in the stratum corneum from 2 - 5 % and varies amongst different anatomical sites (Lampe et al., 1983). Based on reported weight percentages of cholesterol and cholesterol sulfate found in the stratum corneum, we have chosen a 1:5 ratio of cholesterol sulfate:cholesterol to represent normal stratum corneum and a 1:1 ratio to represent abnormal stratum corneum. These values closely reflect the five-fold increase in cholesterol sulfate and 50 % decrease in cholesterol found for recessive x-linked ichthyosis scale (Williams and Elias, 1981; Williams, 1992). In addition we have prepared LUVs without cholesterol sulfate present for comparison with cholesterol sulfate-containing LUVS.

As discussed earlier, EM studies of intact normal stratum corneum show that the lipids in this layer of the skin form intact lamellar sheets (Elias and Friend, 1975; Madison et al., 1987). Thus, *in vitro* studies involving the interaction of stratum corneum lipids of precise lipid composition assembled in unilamellar form (LUVs) may be one way to model the *in vivo*

physical state of the lipids in the stratum corneum. We have chosen widely used membrane fusion assays to study lipid interactions. Membrane fusion is defined as a process by which "the membrane of two lipid vesicles become one and the aqueous contents in them are free to intermix" (Szoka, 1987). Several assays for monitoring fusion have been developed recently. A change in vesicle size can be followed by EM, light scattering, gel filtration and $^{1}H$ NMR (Szoka, 1987). In addition, several investigators have used assays based on the release of encapsulated compounds to monitor vesicle content leakage, a process which is related to fusion kinetically. These leakage assays typically involve monitoring increases in fluorescence intensity when a fluorophore, which is encapsulated inside vesicles either at sufficiently high concentrations or with a high enough concentration of quencher molecules to exhibit intensity quenching, is released from the vesicle and the quenching is relieved due to concentration dilution. Examples of leakage systems include the encapsulation of carboxyfluorescein at a self-quenching concentration inside the vesicles (Weinstein et al., 1977), or the coencapsulation of a water soluble fluorophore, such as 1-aminonapthalene-3,6,8-trisulfonic acid (ANTS), and quencher, such as p-xylylenebis(pyridinium) bromide (DPX) inside the vesicles (Smolarsky et al., 1977; Ellens et al., 1984; Szoka, 1987). Also, lipid monolayer mixing can be monitored by EPR or by fluorescence methods such as the resonance energy transfer (RET) assay, where donor and acceptor fluorescent lipid molecules which are initially in the same vesicles are diluted into unlabeled vesicles. When the bilayers of the vesicles mix, the surface density of probes is reduced, and the fluorescence intensity increases (Struck et al., 1981). Additionally, there are assays based on aqueous contents mixing which involve monitoring enzymatic reactions, chemical complexation or fluorescence

quenching events which occur when two populations of vesicles containing different encapsulated materials in their aqueous phases mix their contents (Szoka, 1987). The ANTS/ DPX methodology has also been applied to the aqueous contents mixing assay, where ANTS and DPX are separately encapsulated in different populations of vesicles. The fluorescence from ANTS becomes quenched when the aqueous contents of ANTS and DPX vesicles mix (Ellens et al., 1985).

Investigations have been carried out on the use of vesicles composed of stratum corneum lipids to study fusion under a variety of different conditions. The majority of these studies utilized electron microscopy techniques to observe changes in SUVs composed of various percentages of epidermal ceramides, cholesterol, cholesterol sulfate and free fatty acids in response to the addition of corneocytes (Abraham and Downing, 1990), salt (Abraham and Downing, 1990), acylceramides and acylglucosylceramides (Abraham et al., 1988a and b) and calcium (Abraham et al., 1987). Additionally, calcium effects are also compared for SUVs prepared with either no free fatty acids or no cholesterol sulfate. The study with corneocytes and SUVs also monitors carboxyfluorescein leakage (Abraham and Downing, 1990). In an altogether different type of study, membrane fusion is explored as a function of temperature and pH on a 1:1:1 mixture of bovine brain ceramide:cholesterol:palmitic acid LUVs by freeze fracture EM and the RET assay for bilayer mixing using phospholipid fluorescent probes (Ahkong et al., 1992). All of these studies did not focus on the lipid composition of diseased stratum corneum. Also, the studies by Abraham and coworkers mentioned above, which have cholesterol sulfate in their lipid composition, did not use LUVs as their model membranes.

In our studies, we have applied ANTS/DPX fluorescence assays for LUV leakage and aqueous contents mixing studies. These assays, which have been developed to monitor changes in phospholipid vesicles (Ellens et al., 1984 and 1985), have not been applied to non-phospholipid based systems in the literature. Therefore, we have characterized our ANTS/DPX probe containing SC LUVs for size and size dispersity, ANTS binding to SC LUVs, and ANTS quenching by DPX. By using well-characterized vesicles in our studies, we can define the composition and morphology of our system for molecular interpretation of our results. The use of both leakage and contents mixing assays allows us to better understand the bilayer lipid interactions. We have monitored the time-dependent changes in the fluorescence of probe-containing LUVs in response to addition of calcium and decrease in pH (from pH 9 to pH 6). We have chosen to monitor pH-induced changes at pH 6 since the skin surface is slightly acidic. Our results demonstrate lipid composition-dependent differences in contents mixing and leakage and differences in pH and calcium effects.

# CHAPTER II

# MATERIALS and METHODS

## 2.1 Materials

All glassware was acid washed and rinsed with deionized water. Cholesterol, cholesterol sulfate, bovine brain ceramides types III and IV (containing alpha-hydroxy acids), lignoceric acid, octacosanoic acid, and dipalmitoylphosphatidylcholine (DPPC) were purchased from Sigma Chemical Co. (St. Louis, MO) and palmitic acid was purchased from Fisher Scientific (Pittsburgh, PA) with at least 99% purity and used without further purification. 8-Aminonaphthalene-1,3,6-trisulfonic acid disodium salt (ANTS) and p-xylylenebis(pyridinium) bromide (DPX) were from Molecular Probes, Inc. (Junction City, OR). Calcium chloride was from Spectrum (Gardena, CA). Other chemicals used to prepare buffers were purchased from Sigma, Fisher or Calbiochem (La Jolla, CA). Borate buffer from Fisher, which was labeled as 0.1 M boric acid-KCl-NaOH at pH 9 (Fisher borate buffer), was used.

## 2.2 MLVs

The weight percentages of lipids found in the stratum corneum: 55 % ceramides, 25 % cholesterol, 15 % free fatty acids and 5 % cholesterol sulfate (Wertz et al., 1987; Abraham, 1992) were used to prepare MLVs. In this study, we used ceramides types III and IV (3:2

weight ratio) to represent ceramides, and palmitic, lignoceric, and octacosanoic acids (1:2:1 weight ratio) to represent free fatty acids. The lipids were solubilized in a chloroform and methanol mixture (2:1 volume ratio). The solvent was then removed with nitrogen gas followed by pumping under vacuum overnight to deposit a lipid thin film on a round bottom flask. Fisher borate buffer (3 ml for 15 mg total lipid) and a few glass beads were added to the lipid film, followed by hand-swirling, vortexing, and heating to 70 °C in a water bath to give MLVs at pH 9.

## 2.3 LUVs

LUVs in Fisher borate buffer were prepared from fresh MLVs by extrusion methods (Hope et al., 1985) at 70 °C with a lipid extruder (Lipex, Vancouver, B.C. Canada). The lipid concentrations in MLVs were usually about 5 mg/ml, but higher concentrations, up to 20 mg/ml, were also used. The MLVs were subjected to five freeze-thaw cycles prior to extrusion (Mayer et al., 1985). Polycarbonate filters (Costar Nucleopore Cambridge, MA) with 5, 1, 0.4 and 0.1 μm pore sizes were used in the extruder in the order listed (Abraham, 1992) to give stable LUVs at pH 9.

Buffers at different pH values were prepared with osmolality values matching the value of Fisher borate buffer (150 ± 10 mmol/kg), measured with a Vapor Pressure 5500 Osmometer (Westcor, Logan, UT). A borate solution (7.5 mM sodium tetraborate, 60 mM KCl, 0.2 mM EDTA) was prepared and titrated with concentrated HCl to either pH 7.4 or 6.0. Sodium phosphate (72 mM) buffer at pH 7.4 was also prepared.

To better compare the properties of LUVs at different pH values, LUVs at 10 mg/ml

were prepared and diluted to about 1 mg/ml with Fisher borate buffer at pH 9. Different portions (generally 2 ml) of the batch were dialyzed with different buffers (borate at pH 7.4 or 6, or phosphate buffer at pH 7.4) at 500-fold excess volume. The pH of the LUV solution inside the dialysis tubing (14K MWCO, from Spectrum Medical Industries, Houston, TX) was checked, and it was found that about 3 h were needed for pH equilibration with borate solution and about 1 h with phosphate buffer. The pH values of all LUV samples (~1 mg/ml) were measured periodically after dialysis, for 24 h. We also measured the pH of LUV samples after the samples were subjected to freeze/thaw cycles immediately after dialysis.

## 2.4 Lipid Composition Determination

The lipids in the vesicle suspensions were extracted using chloroform, methanol and Fisher borate buffer (1:1:1 volume ratio). Potassium chloride (0.1 M) was added to insure that all cholesterol sulfate was recovered in the chloroform phase (Williams and Elias, 1981). Additional potassium chloride was added, if necessary, to help separate the phases. The lipid compositions in the chloroform extracts of MLVs and LUVs were determined by high performance thin layer chromatography (HPTLC) on silica gel 60 plates (E. M. Separations, Gibbstown, NJ). The plates (10 x 20 cm) were developed, charred (Melnik et al., 1989) and scanned with a TLC Scanner II (CAMAG, Muttenz, Switzerland) interfaced to a CR3A Cromatopac Integrator (Shimatzu Corp., Kyoto, Japan). The peak area of each spot in a MLV sample was correlated with the known mass of the corresponding lipid in MLVs. This mass over peak area ratio was then used to convert the peak area of the corresponding LUV lipid spot to lipid mass. This conversion process was necessary since the lipids used did not

char to the same extent to give the same linear relationship between spot intensities and masses for all lipids. The total mass of all the lipids in the LUV sample was obtained from the sum of individual lipid masses. The value of this sum divided by the total MLV lipid mass represented the recovery of lipid after extrusion. The LUV lipid composition was then determined from the values of individual and total masses in the LUV sample.

## 2.5 Vesicle Size

Freeze-fracture and cryo-EM were performed by Northern Lipids Inc. (Vancouver, B.C. Canada), as a service, on LUVs (20 mg/ml) in Fisher borate buffer at pH 9.

Photon correlation spectroscopy of QELS measurements with a particle size analyzer (BI 90; Brookhaven Instruments, New Haven, CT) was used to determine the hydrodynamic effective diameters of the LUVs in different buffer systems. Immediately after dialysis, LUV samples (5 - 10 mg/ml) were diluted 2 to 10-fold as necessary to bring the photon count rate within the recommended range (250-500 kcps) for vesicles with effective diameters of 100 - 300 nm. At least two different lipid concentrations were used for each sample to show that the diffusion coefficient of the sample did not change on dilution. Typically 7,500 cycles (6.25 min) were used. The dust cutoff for the instrument was kept constant for all samples. If the dust factor in a sample was > 0.02, the measurements were rejected. For QELS measurements carried out continuously over 24 h, the LUVs in the cuvette were kept at 25 °C in the instrument throughout the entire measurement period. The sampling time was 25 min (30,000 cycles). Cumulant analysis was applied to scattering data to give effective diameters and polydispersity. If the polydispersity of an LUV sample was greater than 0.11,

the QELS measurements of this sample were not used, and the sample was also not used for preparing LUVs at different pH values. To further determine whether the diameter distribution was a broad unimodal or a skewed, multimodal distribution, inverse Laplace transform analysis, employing an exponential sampling technique, was also used. This analysis, however, gave a less rigorous analysis of the particle size. Thus we used the effective diameter from cumulant analysis as the size of the samples.

## 2.6 DSC

Lipid thin films, similar to those used for MLVs, were scraped from the walls of a round bottom flask and sealed in an aluminum sample pan. The sample (3 - 4 mg) was then equilibrated to 5 °C in a differential scanning calorimeter (DSC 2910; Thermal Analysis Instruments, New Castle, DE). The sample was initially heated from 5 to 90 °C at a rate of 2 °C/min and then cooled back to 5 °C at the same rate. Heat flow (thermogram) was then recorded during the second heating process. Thermograms were also obtained during the third cooling and heating processes to determine whether the observed thermal transitions were reversible. Most samples were used immediately after they were transferred to sealed sample pans. Some samples remained in the sealed pans for a longer period of time, but less than 24 h. No differences in the second heating thermograms were observed in samples used.

## 2.7 Spin Labeled LUVs

Two fatty acid spin probes, 5-doxylstearic acid (5-DSA) and 12-doxylstearic acid (12-DSA) were purchased from Molecular Probes (Eugene, OR) or Syva (Palo Alto, CA) and

used without further purification. 5-DSA or 12-DSA in ethanol was dried to a thin film with a gentle stream of nitrogen gas. A sample of LUVs at pH 9 was then added to the spin label thin film at a lipid-to-spin label molar ratio of ~ 150 to avoid spin-spin exchange (Fung and Johnson, 1984). The spin label concentrations in samples were generally about 7 - 8 x $10^{-5}$ M. The spin label was also directly incorporated into the lipid thin film by adding the spin label in ethanol to the lipids in chloroform-methanol prior to nitrogen gas evaporation. No significant spectral differences were found by the two different labeling methods. Samples of spin labels in borate buffer (~ 2 x $10^{-5}$ M) were used as controls and were prepared in tandem with the spin labeled LUV samples.

## 2.8 EPR Measurements

EPR measurements were performed using a Varian E-109 EPR Spectrometer equipped with an IBM variable temperature control unit (Fung and Zhang, 1990). One gauss modulation, 60 s scan time and 5 mW microwave power were used to obtain EPR spectra. The EPR cavity with a standard quartz EPR tube filled with silicone fluid to provide thermal stability was pre-warmed to a desired temperature, which was monitored by a copper-constantan thermocouple (Fung and Zhang, 1990). The spin labeled LUV sample was placed in the cavity for 2 min before data acquisition to assure thermal equilibration. After each EPR measurement, the sample was removed from the cavity and placed in a water bath at the same temperature until the cavity reached a new temperature equilibrium. Temperatures from 25 to 90 °C were used.

## 2.9 EPR Data Analysis

### 2.9.1 Spectral Subtraction

Spectral subtraction, using commercially available software ASYST (Mac Millan Software, New York, NY.), modified for EPR operation, was performed to deconvolute the fast (weakly immobilized) and slow (strongly immobilized) components in spin labeled LUV spectra (Fig. 1A). We were able to use the spectra of spin labels in buffer at matching temperatures (Fig. 1B) to remove the weakly immobilized component in the spectra of labeled LUVs at all temperatures studied to give the spectra of the slow component (Fig. 1C). A second subtraction provided the spectra of the fast component. This spectral subtraction procedure allowed us to use the composite spectra of LUVs to provide pairs of two single-component deconvoluted spectra for more vigorous analysis of spectral parameters, such as the intensity/concentration of each component in the LUV samples.

### 2.9.2 Spin Label Intensity

Spectra of a spin label in buffer at different temperatures were obtained, and results of double integration of the spectra were used to provide calibration curves for spin label intensity at different temperatures. Such procedures were required to account for differences in signal intensity due to dielectric-induced changes in cavity sensitivity at different temperatures (Fung and Johnson, 1983). For 5-DSA intensity measurements, the peak height of the central line of the weakly immobilized component was also used to estimate concentration since some samples exhibited low signal-to-noise ratio of the weakly immobilized component signal yielding unreliable double integration results.

### 2.9.3 Hyperfine Splitting

The hyperfine splittings ($2A_{max}$) of the strongly immobilized component in LUV spectra were measured as the distance between the outermost EPR lines (Griffith and Jost, 1976).

### 2.9.4 Rotational Correlation Time

The rotational correlation times for the weakly immobilized signal in LUVs and for the strongly immobilized signal for 12-DSA in LUVs at 90 °C were estimated from line-width and line height measurements using the linear terms of the motional narrowing theory (Fung and Johnson, 1984). Approximate axial correlation times ($\tau_R^z$) for the remaining strongly immobilized signals were obtained from the following expression which includes the temperature dependence of the hyperfine separation measurements (Johnson, 1979):

(1) $$(\tau_R^z)^{-1} = a_z(T)[1 - A_{zz}^*/A_{zz}^0(T)]^{bz}.$$

For simplicity, we used this equation to estimate the rotational correlation times. Due to anisotropic averaging, more quantitative calculations of the rotational correlation times should be obtained with the spectral simulation methods provided by Freed and coworkers (Freed, 1976).

### 2.9.5 Partition Ratio

The partitioning of fatty acid spin labels in aqueous and lipid phases in LUV samples was followed as a function of temperature. The fraction of spin labels in the aqueous phase of LUV samples ($f_{AQUEOUS}$) at a particular temperature was obtained from the spin label

Figure 1 **A Typical Example of the Results from Spectral Subtraction of 5-DSA Spin-Labeled LUVs into Strongly and Weakly Immobilized Components.** Shown in the figure are EPR spectra at 77 °C of (A) 5-DSA in LUVs in Fisher borate buffer at pH 9 with a lipid-to-spin label molar ratio of 150 and a spin label concentration of ~ 4 x $10^{-5}$ M and (B) 5-DSA dispersed in the same buffer. The weakly immobilized component in (A) was removed by spectral subtraction of (A) - (B) to give the spectrum of spin label fraction that was intercalated in the lipid phase of LUVs (C).


A
B
C

intensities of deconvoluted spectra of the weakly immobilized signal, and the fraction of spin labels in the lipid phase ($f_{LIPID}$) was obtained from the corresponding spectra of the strongly immobilized signal. The ratios of these two fractions ($f_{LIPID}/f_{AQUEOUS}$) at a particular temperature were calculated. This ratio is directly related to the partition coefficient, partial specific volume of lipid and lipid concentration (Miyazaki et al., 1992).

## 2.10 Preparation of SC Lipid LUVs Containing ANTS and/or DPX

Multilamellar vesicles (MLVs) and extruded large unilamellar vesicles (LUVs) were prepared at a lipid concentration of 5 mg/ml for all experiments unless otherwise noted. The lipid composition of the LUVs was varied as shown in Table 1. Repeated extrusions were made through the 0.1 μm filters , with frequent filter change as necessary to keep the applied pressure < 250 psi, until the optical absorbance at 700 nm ($A_{700}$) was < 0.250. Samples for leakage and aqueous contents mixing experiments were prepared with ANTS and/or DPX (Ellens et al., 1984 and 1985). LUVs prepared for the leakage assay contained 12.5 mM ANTS and 25 mM DPX in Fisher borate buffer at pH 9. An additional 25 mM KCl was added to maintain an osmolality of ~270 mmol/kg. LUVs prepared for the contents mixing assay contained either (i) 25 mM ANTS or (ii) 50 mM DPX buffered with Fisher borate buffer at pH 9. Since ANTS is extremely acidic, it was necessary to add a small amount of NaOH to the solutions containing ANTS in order to bring the pH back up to 9.0. For the ANTS solution, an additional 52 mM KCl was added and for the DPX solution, an additional 7 mM KCl was added to maintain the solution osmolality at ~270 mmol /kg.

To prepare LUVs for ANTS binding experiments, normal lipid composition SC LUVs

Table 1 Lipid Compositions (Weight %) Used to Make LUVs for Fluorescence Studies

| Composition | Ceramides[a] | Cholesterol | Cholesterol sulfate | Fatty acids[b] |
|---|---|---|---|---|
| 1[c] | 55 | 15 | 15 | 15 |
| 2[d] | 55 | 25 | 5 | 15 |
| 3 | 55 | 30 | 0 | 15 |

[a]Ceramides are composed of a 3:2 weight ratio of bovine brain ceramides type III and IV, respectively.

[b]Fatty acids are represented by 1:2:1 (by weight) palmitic:lignoceric:octacosanoic acids.

[c]This composition reflects the 1:1 cholesterol:cholesterol sulfate ratio observed with the diseased skin state, recessive x-linked ichthyosis.

[d]This composition reflects the normal distribution of lipids in the stratum corneum and is designated normal SC LUVs.

were prepared in Fisher borate buffer at pH 9. DPPC LUVs were also prepared as a control in pH 9 borate column buffer (30 mM boric acid, 0.2 mM EDTA, ~140 mM KCl titrated to pH 9 with 1 N NaOH, osmolality ~270 mmol/kg) by extrusion at 48 °C through 0.4 and 0.1 μm filters.

For quenching experiments, normal lipid composition SC LUVs were coencapsulated with 12.5 mM ANTS and either 12.5, 25, or 45 mM DPX in Fisher borate buffer at pH 9. Additional KCl was added to make the LUVs isosmotic. DPPC LUVs were also prepared as a control under the same encapsulation conditions at pH 9.

For all LUVs prepared with ANTS and/or DPX solutions, the LUVs were separated from unencapsulated material by passing 1.5 ml of the mixture through a Sephadex G-75 (Pharmacia, Piscataway, NJ) column (1.7 cm x 22 cm) equilibrated with borate column buffer. The LUV peak was eluted from the column in the void volume. Approximately 4.5 ml associated with the LUV peak were pooled. This diluted sample (~1 mg/ml total lipid) was used for experiments. Samples were stored, sealed in the dark, until use.

## 2.11 Lipid Concentration Determination of ANTS/DPX SC LUVs by Cholesterol Oxidase

The cholesterol concentration in the fluorescent probe-containing SC LUV samples after column separation was determined via the cholesterol oxidase assay (Barenholz et al., 1978). A standard curve for determining the cholesterol content was generated using cholesterol samples with known weights between 1 and 50 μg. Samples were run with and without cholesterol sulfate present to determine whether cholesterol sulfate interfered with the assay. Assuming that the decrease in cholesterol concentration reflects the decrease in

concentration of total lipid, due to the extrusion technique and dilution through the column, the concentration of total lipid was calculated from the cholesterol concentration in the dilute sample.

## 2.12 Lipid Composition of ANTS/DPX SC LUVs

The lipids in 25 mM ANTS LUVs after column elution were extracted into organic solvent as previously described (Section 2.4). The lipid composition of SC LUVs, containing 0, 5 or 15% cholesterol sulfate with other lipids present in the quantities described in Table 1, was determined by HPTLC on silica gel 60 plates. A control sample (7 mg/ml) containing 1 mg of each of the seven lipids used to make the LUVs was included.

## 2.13 Vesicle Size Determination of ANTS/DPX LUVs

Quasi-elastic light scattering measurements with cumulant analysis were performed on encapsulated LUVs to determine effective diameter and polydispersity as described in Section 2.5.

To investigate the effect of fluorescence probe concentration on SC LUV effective diameter and polydispersity, normal (5% cholesterol sulfate) SC LUVs encapsulated with 12.5, 25 or 50 mM ANTS and 25, 50, or 90 mM DPX were prepared at pH 9 in borate buffer. KCl was added to each solution to bring the osmolality to ~270 mmol/kg. After separation of free ANTS or DPX from the LUVs, the effective diameter and polydispersity of the preparations were determined by QELS.

To determine whether increased salt concentration affects the effective diameter and

the polydispersity of SC LUVs, normal SC LUVs in Fisher borate buffer with 60 mM KCl added (osmolality ~255 mmol/kg) were also prepared for QELS measurements.

## 2.14 Conditions for Fluorescence Measurements of Binding, Quenching, Contents Mixing and Leakage

For all experiments, fluorescence was measured with a Hitachi F2000 Fluorescence Spectrophotometer (Tokyo, Japan) equipped with a circulating water bath set at 25 °C. Excitation was at 384 nm and emission was measured at 540 nm through a Corning 3-69 cutoff filter to help eliminate the effect of light scattering (Ellens et al., 1984). For all experiments, 1.5 ml of sample was measured in a stirred cuvette. The shutter was activated between measurements to help reduce photobleaching. Samples not being measured were stored in the dark until use and then stirred before measurement.

## 2.15 Binding of ANTS to LUVs

The binding of ANTS to LUVs (Ellens et al., 1984) was determined by incubating empty LUVs (5 mg/ml in borate column buffer at pH 9) with 25 mM ANTS , 30 mM boric acid, 112 mM KCl, and 0.2 mM EDTA buffered at pH 9 in a 1:1 volume ratio for 1 hour at room temperature. The LUVs in the mixture were separated from free ANTS on a Sephadex G-75 column. The fluorescence associated with the LUV peak was measured and compared to the fluorescence intensity of LUVs encapsulated with ANTS. The binding experiments were performed with normal (5% cholesterol sulfate) SC LUVs, and DPPC LUVs run as a control.

## 2.16 Concentration Dependent Quenching of Fluorescence

The quenching of ANTS fluorescence by DPX in LUVs was measured by coencapsulating 12.5 mM ANTS with 12.5, 25 or 45 mM DPX in LUVS. The fluorescence intensity of 1.5 ml of LUVs (~1 mg/ml) was measured and designated as the residual fluorescence. The total fluorescence intensity of 1.5 ml of LUVs lysed with 0.5% (by vol.) Triton X-100 was set as 100% (maximal) fluorescence. The quenching was determined as:

(2) % quenching = 100 - (100 x residual fluorescence/ maximal fluorescence)

Quenching experiments were performed on column separated normal (5% cholesterol sulfate) SC LUVs and DPPC LUVs at ~1 mg/ml.

## 2.17 Leakage Assay

### 2.17.1 pH 9

The fluorescence intensity of 12.5 mM ANTS/ 25 mM DPX SC LUVs (1.5 ml; ~1 mg/ml total lipid) was monitored for 5 hours. Three 5 second readings were averaged together as one time point measurement.

### 2.17.2 pH 6

ANTS/DPX LUVs (1.5 ml; ~1 mg/ml) were dialyzed for 45 min against a 500-fold (by volume) excess of 2-[N-Morpholino]ethanesulfonic acid (MES) buffer at pH 6 (30 mM MES, 0.2 mM EDTA, ~140 mM KCl, pH 6, osmolality ~270 mmol/kg) at ambient temperature. The contents of the dialysis tubing (14K MWCO from Spectrum Medical Industries, Houston, TX) were removed and the fluorescence intensity of the sample was

measured initially and over a five-hour time period. Three 5 second readings were averaged together for one time point. Alternatively, the pH of normal lipid composition ANTS/DPX LUVs (pH 9) was lowered by injecting 50 µl of 1M MES acid into the LUVs (final concentration of MES is 33 mM). Time points were taken over a 5-hour time period.

2.17.3 5 mM $Ca^{2+}$

The fluorescence intensity of ANTS/DPX LUVs (1.5 ml; ~1 mg/ml) was measured at pH 9. To a stirring cuvette of LUVs, 15 µl of $CaCl_2$ solution (0.5 M) was added. The fluorescence intensity was recorded every 5 seconds for about 2 min and then periodically over 5 hours.

2.17.4 Determination of Maximum Fluorescence, Residual Fluorescence, and Leakage

Leakage was measured as % maximum fluorescence where:

(3) $$\% \text{ maximum fluorescence}(t) = 100 \times (F(t)-F(0))/(F_{max}-F(0))$$

and F(t) is the fluorescence emission intensity at time t, F(0) is the initial fluorescence intensity (t = 0 h) designated as residual fluorescence intensity, and $F_{max}$ is the maximum fluorescence intensity obtained by lysing the vesicles with Triton X-100 (0.5 % by volume) after the experiment was completed.

2.18 Aqueous Contents Mixing Assay

2.18.1 pH 9

ANTS (25 mM) LUVs and DPX (50 mM) LUVs were mixed in a 1:1 ratio (1.5 ml;

~1 mg/ml total lipid). The fluorescence intensity of the sample was monitored over 5 hours.

2.18.2 pH 6

ANTS LUVs (0.75 ml) and DPX LUVs (0.75 ml) were separately dialyzed against a 500-fold excess of MES buffer as stated above for leakage samples. The contents of each dialysis tubing were mixed, and the fluorescence intensity was monitored initially and over a five-hour time period. Alternatively, the pH of normal lipid composition ANTS and DPX LUVs was lowered by injecting 50 µl of 1 M MES acid into 1.5 ml of a 1:1 mixture of ANTS and DPX LUVs (final concentration of MES is 33 mM). Time points were taken over a 5-hour time period.

2.18.3 5 mM $Ca^{2+}$

ANTS and DPX LUVS were mixed in a 1:1 ratio (1.5 ml; ~1 mg/ml total lipid). Calcium was added to give a 5 mM final concentration and the fluorescence intensity recorded as described for the leakage samples.

2.18.4 Determination of Aqueous Contents Mixing

Aqueous contents mixing was expressed as % maximum fluorescence where:

(4) $$\% \text{ maximum fluorescence} = 100 - (100 \times F(t)/F(0))$$

and F(t) is the fluorescence emission intensity at time t and F(0) is the initial fluorescence intensity which is designated as the maximum fluorescence.

## 2.19 Data Analysis from Fluorescence Assays

Plots of % maximum fluorescence vs. time were generated with the technical graphics and data analysis program, Origin (Microcal Software, Inc., Northampton, MA). Approximately three runs of data were acquired for each experimental condition with the three lipid compositions used. Since data of different runs were not obtained with the same time points, each run of data was separately best fitted to a randomly selected equation which resulted in the maximum number of points falling on the curve. With this equation, 101 data points equally spaced from 0 to 5 h were selected for averaging with other similarly fitted data points from other runs. These mean values of % $F_{max}$ were plotted as a function of time, with standard deviations calculated at every 0.5 h. Data points at 0.05 and 0.25 h were also included to better define the curve during the initial 30 min of measurements. For most of the conditions, data could be fitted with a four-parameter ($B_1$, $B_2$, $k_1$ and $k_2$) equation:

(5) $$\% F_{max} = (B_1 + B_2) - B_1e^{-k_1t} - B_2e^{-k_2t}$$

where t = time in h.

There were two exceptions to the use of this equation for curve fitting. The data from the pH 6-induced leakage of SC LUVs containing no cholesterol sulfate could be fitted not by equation 5, but by a three-parameter ($A_o$, $k_1$ and $k_2$) equation:

(6) $$\% F_{max} = [A_o/(k_2-k_1)]\,[k_2(e^{-k_1t} -1) - k_1(e^{-k_2t} - 1)].$$

Also the data from the leakage of SC LUVs at pH 9 fit a single parameter equation of the form:

(7) $$\% F_{max} = Bt.$$

All chosen equations allow that % $F_{max}$ = 0 when t = 0.

# CHAPTER III

# RESULTS

## 3.1 Lipid Composition, Vesicle Size and Stability of LUVs at pH 9

The lipid composition found in the stratum corneum (Wertz et al., 1987) was used to prepare MLVs. The HPTLC results of MLV and LUV lipids (Fig. 2) were very similar. The two spots at the top of the plate were assigned to free fatty acids (octacosanoic, lignoceric and palmitic acids), followed by cholesterol, ceramide type III, ceramide type IV and cholesterol sulfate. Scanning densitometry scans on the charred spots from three separate preparations showed 80 - 95 % recovery of the MLV lipids in the LUV samples. Thus, the LUV preparation procedures described above gave relatively high yields of LUVs. In addition, the lipid compositions of MLVs and of LUVs (Table 2) were nearly the same. Little detectible lipid degradation or loss of specific lipid occurred as a result of either the heating or the extrusion process used in sample preparation. Thus, the lipid composition of LUVs was very similar to the one designated to represent stratum corneum lipid composition.

The micrographs of LUVs at pH 9 using either freeze fracture EM (Fig. 3A) or cryo-EM (Fig. 3B) demonstrated, independently, that the LUVs were predominantly spherical with average diameters of about 100 nm. Some of the vesicles also displayed an angular profile by both EM techniques, which has been observed in the presence of long, saturated acyl chains of phospholipid vesicles (Klösgen and Helfrich, 1993; personal communication, T.

Figure 2 **High Performance Thin Layer Chromatogram of Stratum Corneum Lipids in MLVs and LUVs with 50 μg Total Lipid for Each Sample.** The silica gel 60 plate was first developed with chloroform:methanol:water (95:20:1 by volume) to 6.5 cm above the origin and then with hexane:diethyl ether:acetic acid (80:20:10 by volume) to ~12 cm above the origin. The plate was sprayed with 10 % (w/v) cupric sulfate hydrate in 8 % (w/v) phosphoric acid and charred at 170 °C for 60 min for visualization. The densitometric scan of the MLV lane is shown on the left. The peak positions are not matched to the spot positions on the plate due to limited selection on chart speed used for the densitometer. The identification of each lipid spot was made with similar chromatograms of known lipid and is shown.

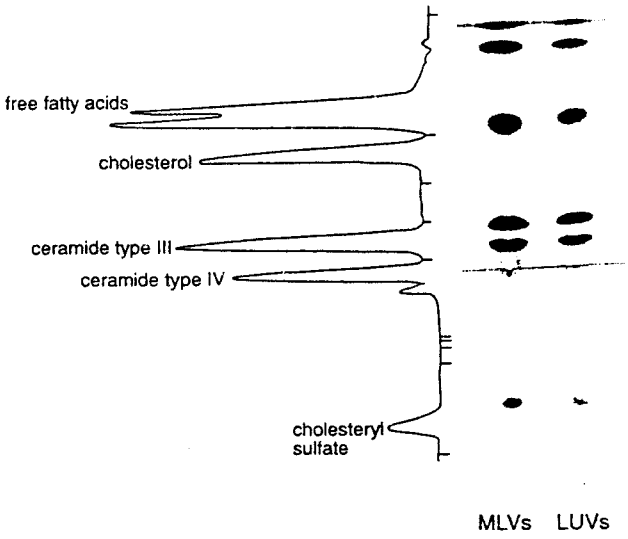
free fatty acids
cholesterol
ceramide type III
ceramide type IV
cholesteryl sulfate
MLVs
LUVs

Table 2 Lipid Composition (Weight Percent, %) in Multilamellar Vesicles (MLVs), and in Extruded Large Unilamellar Vesicles (LUVs)

| Lipid Type | MLV (%) | LUV (%) |
|---|---|---|
| Free Fatty Acid | 15* | 15.5 ± 1.7‡ |
| Cholesterol | 25 | 25.5 ± 1.9 |
| Ceramide III | 33 | 33.2 ± 1.0 |
| Ceramide IV | 22 | 20.9 ± 0.9 |
| Cholesterol Sulfate | 5 | 5.0 ± 1.2 |
| Total | 100 | 101 |

*14 μg of total lipid were used in two runs and 25 μg in the third run.

‡Average weight percent of three different runs.

The intensities of the spots on the HPTLC plate, as shown in Fig. 2, were converted to weight percent for each lipid type, using MLV spot intensities as reference. See text for details.

Figure 3 **(A) Freeze-Fracture and (B) Cryo-Electron Micrographs of LUVs at 20 mg/ml in Fisher Borate Buffer.** The scale bars are 200 nm. The vesicles are generally spherical with a diameter of about 100 nm. The micrographs were prepared, as a service, by Northern Lipids Inc. (Vancouver, Canada).

A.

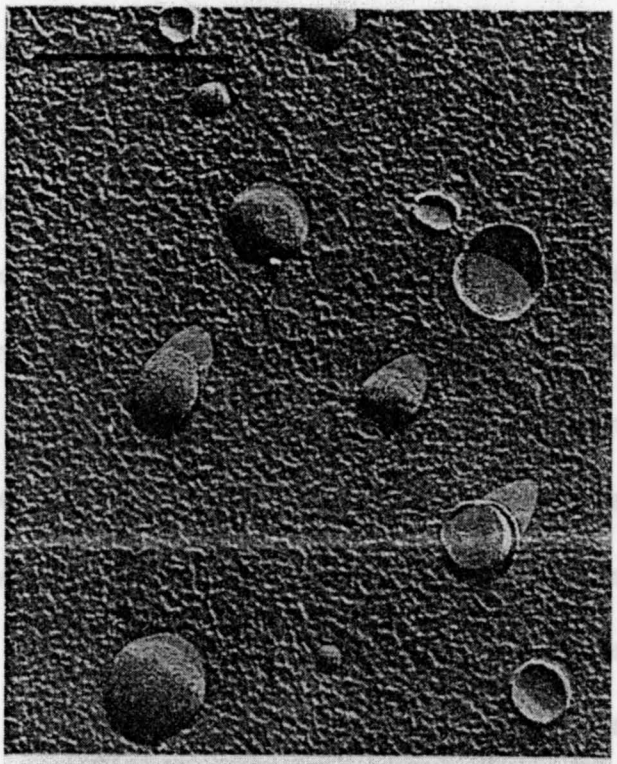

B.

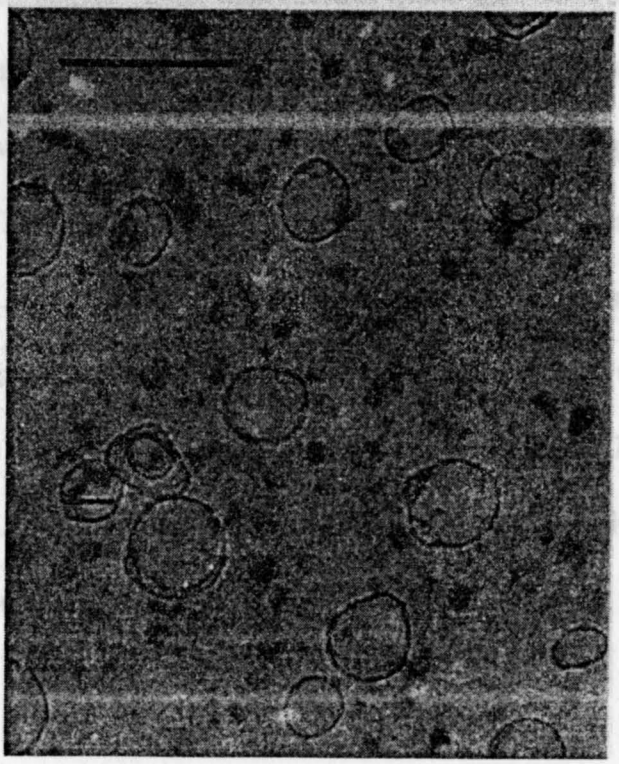

Madden, Northern Lipids Inc.). There was a tendency for the vesicles to aggregate at the high lipid concentrations (20 mg/ml) used for EM measurements.

The average effective diameter from cumulant analysis of QELS measurements of LUVs obtained from 16 separate LUV preparations, including the 4 different preparations shown in Table 3, was 119 ± 10 nm with a polydispersity of 0.086 ± 0.019. The standard deviation of 10 nm reported with the average effective diameter was mostly due to slightly different diameters of LUVs obtained from different LUV preparations. The standard deviation of multiple QELS measurements on a single LUV sample was equal to or less than 1 nm. Since the majority of the vesicles in micrographs appeared spherical, the effective diameters obtained from cumulant analysis should be fairly accurate, since the analysis assumed particles to be spheres. Polydispersity values provided information on the relative width of the diameter distribution. Samples with values below 0.08 were considered to have diameters narrowly distributed. Thus, both EM and QELS data showed that the LUVs at pH 9 had shapes similar to spheres with diameters rather narrowly distributed around 100 - 120 nm. These LUVs were also quite stable upon storage at room temperature. The average effective diameter of LUVs after 48 h storage remained at about 114 nm with a polydispersity of 0.076. Inverse Laplace transform analysis showed a single population of LUVs with a diameter centered around 116 nm for the time period studied. Thus, the effective diameters of LUVs remained narrowly centered around 114 nm after 48 h of storage at room temperature. The LUV samples (1 mg/ml) remained free of precipitation for 4 - 6 weeks, suggesting that these vesicles were very stable at room temperature.

Table 3 QELS Particle Size Analysis (Using Both Cumulant and Inverse Laplace Transform Analysis Methods) of LUVs in Borate Buffer at Different pH Values and in Phosphate Buffer at pH 7.4, with Measurements Taken Immediately after Dialysis (Top Panel) and 48 h Later (Bottom Panel).

| | | | | Inverse Laplace transform analysis | | | |
|---|---|---|---|---|---|---|---|
| | | Cumulant analysis | | Population 1[c] | | Population 2 | |
| Buffer | pH | ED[a] (*n*) | PD[b] | D (*n*)[d] | Fraction (%)[e] | D (*n*) | Fraction (%) |
| Borate | 9 | 114 ± 13 (4) | 0.091 ± 0.014 (4) | 116 ± 13 (4) | 100 | ND[f] | ND |
| Borate | 7.4 | 117 ± 11 (4) | 0.137 ± 0.035 (4) | 97 ± 26 (4) | 32 - 100 | 226 ± 121 (3) | 0 - 68 |
| Borate | 6 | 128 ± 16 (5) | 0.177 ± 0.053 (5) | 112 ± 23 (5) | 44 - 100 | 333 ± 171 (3) | 0 - 56 |
| Phosphate | 7.4 | 133 ± 23 (3) | 0.184 ± 0.042 (3) | 128 ± 16 (3) | 100 | ND | ND |
| Borate | 9 | 114 ± 13 (3) | 0.076 ± 0.005 (3) | 119 ± 16 (3) | 100 | ND | ND |
| Borate | 7.4 | 127 ± 11 (4) | 0.165 ± 0.047 (4) | 120 ± 15 (4) | 76 - 100 | 796 ± 100 (2) | 0 - 24 |
| Borate | 6 | NA[g] | NA | NA | NA | NA | NA |
| Phosphate | 7.4 | 140 ± 13 (3) | 0.192 ± 0.042 (3) | 116 ± 9 (3) | 74 - 82 | 592 ± 241 (3) | 18 - 26 |

Table 3 (continued)

[a]ED is the average effective diameter in nanometers of LUV ± SD (*n*, number of different samples used).

[b]PD is the polydispersity (the relative width of the distribution of ED).

[c]Populations 1 and 2 represent the two subpopulations identified by the inverse Laplace transformation analysis.

[d]D is the center diameter (in nanometers) for each subpopulation ± standard deviation (*n*, number of samples with the subpopulation).

[e]Fraction is the intensity-weighted fraction. The value (%) is shown as a range of values obtained from all samples. For example, for LUVs in borate buffer at pH 7.4, in population 1, the % for D = 93, 75, 134, and 86 nm were 73, 32, 100, and 42 %, respectively and the corresponding % in population 2 with D = 366, 146 and 168 nm were 27, 68, and 58 %, respectively.

[f]ND refers to "not detected".

[g]NA refers to "not analyzed", due to large amounts of precipitation (large dust factors) in the sample (see Fig 4).

## 3.2 Effect of pH on Vesicle Effective Diameter and Polydispersity

Upon decreasing the pH values of LUV samples, the average effective diameter of LUVs in borate solution increased slightly, from 114 nm at pH 9, to 117 nm at pH 7.4 and 128 nm at pH 6.0 (Table 3, top panel). The corresponding values for polydispersity increased from 0.091 to 0.137 and 0.177, respectively. Size distribution results from inverse Laplace transform analysis also indicated more than one population. The average diameter in each population exhibited large standard deviations and the intensity-weighted percentages also varied greatly from run to run, suggesting that the size of LUVs in borate buffer at pH 7.4 and 6.0 was somewhat heterogeneous and varied from run to run. Upon storage for 48 h, the LUVs in borate at pH 7.4 further increased their size (127 nm) and heterogeneity (polydispersity = 0.165) (Table 3, bottom panel). For LUVs at pH 6.0, storage for 48 h rendered samples with precipitation. Consequently, large dust factors were obtained for QELS measurements and the data were not analyzed. HPTLC analysis of the precipitated lipid showed the presence of all lipids, suggesting that the LUVs had fallen apart at pH 6 after storage at room temperature for 48 h.

We have also followed an LUV sample at pH 6 immediately after preparation with QELS for about 18 h continuously. As shown in Fig. 4, the effective diameters increased gradually over 15 h, from 112 nm to about 119 nm. The corresponding polydispersity values also increased from 0.145 to 0.196. The dust factors in the sample remained around 0.01, indicating that the sample was still relatively dust-free. After 15 h, the dust factor increased suddenly to about 0.07 at 16 h and 0.12 at 17 h. The effective diameters and polydispersity values both dropped, signifying an onset of drastic changes in the LUV sample, which led to

Figure 4 **QELS Particle Size Analysis of LUVs as a Function of Time.** (A) Effective diameter, (B) Polydispersity and (C) Dust Factor, of LUVs prepared in Fisher borate buffer at pH 9 (open circles) and then dialyzed in 7.5 mM borate buffer containing 60 mM KCl and 0.2 mM EDTA at pH 6 (filled circles) are plotted versus time. The osmolarity of the buffers was 150 ± 10 mOsm. QELS measurements were continuously recorded until the dust factor increased significantly. The total lipid concentration of the sample was approximately 1.3 mg/ml. The sample was kept under atmospheric pressure at 25 °C during measurement. Time zero represents the time when the contents inside the dialysis tubing reached pH 6.

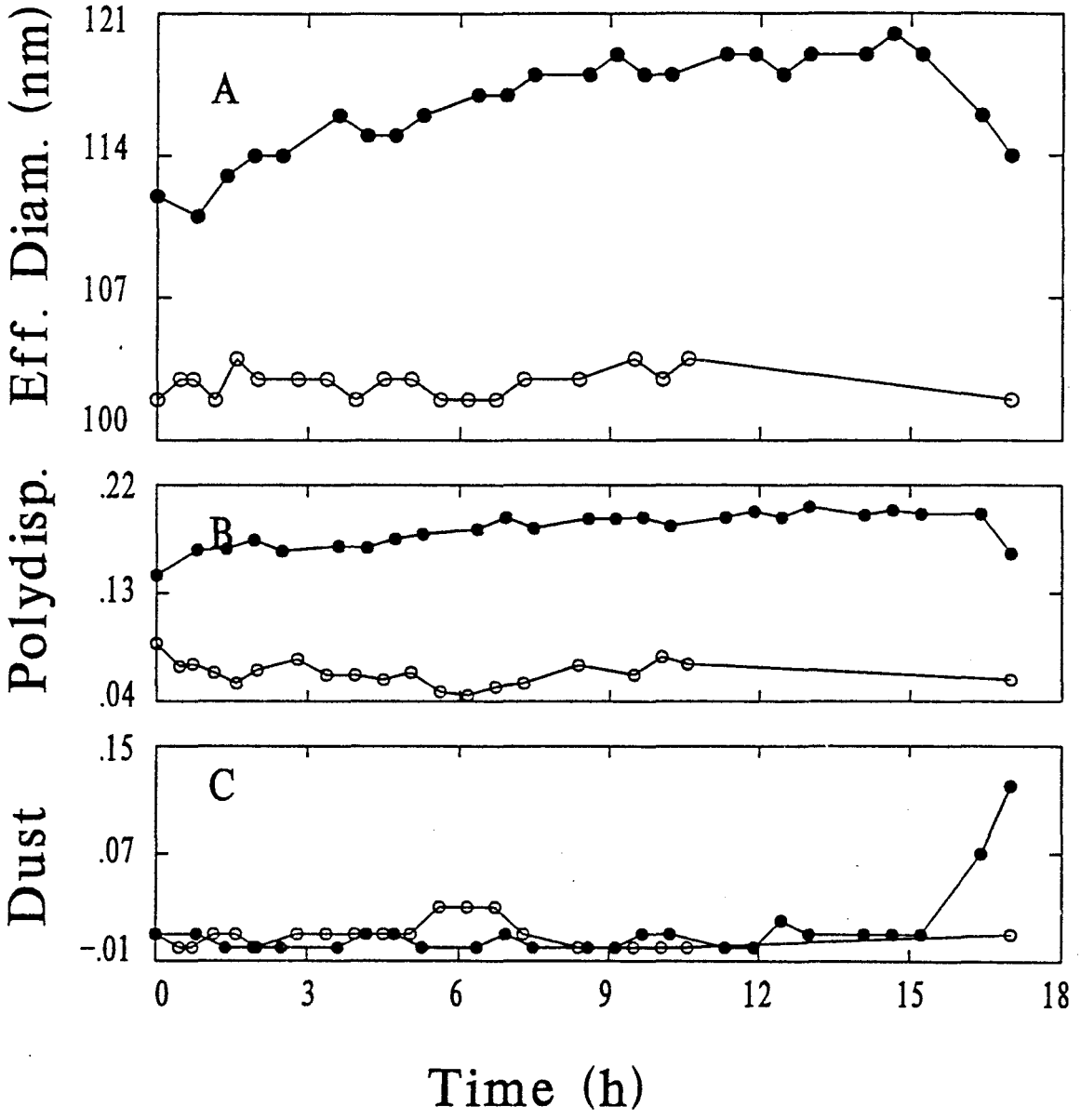
Eff. Diam. (nm)
121
114
107
100
A
Polydisp.
.22
.13
.04
B
Dust
.15
.07
-.01
C
0
3
6
9
12
15
18
Time (h)

the eventual precipitation of LUVs, as shown in samples after storage for 48 h (Table 3, bottom panel). As shown in Fig. 4, QELS properties of the control sample (LUVs at pH 9) remained essentially the same throughout the time period studied.

Since borate buffer has little buffering capacity at pH 7.4 and 6.0, we also dialyzed the pH 9 LUV samples with phosphate buffer at pH 7.4. The effective diameters of LUVs in phosphate buffer were ~ 15 nm larger than those in borate solution at pH 7.4 (Table 3, top panel). The polydispersity values increased from 0.137 to 0.184. Inverse Laplace transform analysis showed one population with an average diameter of 128 nm, in good agreement with results obtained from the cumulant analysis. Thus the LUVs in phosphate buffer at pH 7.4 appeared to have diameters broadly distributed around 130 nm. Upon storage for 48 h, the effective diameters appeared to increase slightly, to about 140 nm. Inverse Laplace transform analysis revealed two populations of different diameters in the LUV samples, with the majority centered around 120 nm and a minor group centered around 600 nm (Table 3, bottom panel). These data suggested that the LUVs in phosphate buffer at pH 7.4 were about 10 - 15 nm larger than those at pH 9 and were not as stable as the LUVs at pH 9.

It should be noted that when the LUVs in borate buffer at pH 9 were subjected to dialysis to pH 7.4 or 6 according to the procedures that we used, the external pH of the LUVs reached the designated pH value. The internal pH values of the LUVs were not necessarily the same as the external pH values. Previous studies of phospholipid vesicles prepared in borate buffer at pH 10.5 and injected into HEPES buffer at pH 7.4 have shown the existence of pH gradient of ~ 3 units across the vesicle bilayer for at least 30 min (Wilschut et al., 1992). It has also been found that borate does not readily permeate phospholipid vesicles

(Eastman et al., 1989). We performed simple pH measurements on our LUV samples at pH 7.4 in both phosphate and borate buffers. While a 0.05 pH unit increase was noted for LUVs in borate at pH 7.4, no detectable change in pH was observed for LUVs in phosphate buffer. For LUVs at pH 6, a 0.40 pH unit increase was measured. Changes similar in pH to those described above were also measured for LUV samples subjected to freeze/thaw cycles immediately after dialysis. The buffers and solutions themselves showed no increases in pH over time. No detectable changes in pH were measured for samples of LUVs at pH 9. It is likely that stratum corneum lipid bilayers also exhibit pH gradients similar to those observed in phospholipid bilayers. More detailed studies are needed for a better understanding of the pH properties of stratum corneum LUVs prepared at pH 9 and dialyzed to pH 7.4 or 6.

## 3.3 Thermal Properties of Lipid Mixtures of LUVs

Second heating thermograms of stratum corneum lipid mixtures with a lipid composition used for LUV preparation showed two broad, enthalpic transitions centered at about 60 °C and at 65 °C , with a shoulder at about 70 °C (Fig. 5). These transitions were also detected in the third heating thermogram, indicating that the enthalpic transitions were reversible. First heating thermograms of some samples exhibited only one broad transition instead of a doublet with variations in the temperature at which the transition was centered (56 - 65 °C). These slight differences could be due to variations in sample preparations, including moisture contents in lipids. Regardless of the variation observed in the thermograms of first heating, the thermograms of the second and third heating were essentially the same.

Figure 5 **Differential Scanning Calorimetry Thermogram of a Typical Stratum Corneum Lipid Thin Film Prepared with a Lipid Composition the Same as that Used to Prepare LUVs.** The thermogram represents the second reheat of the sample at a scan rate of 2 °C/min. The film was evacuated under vacuum pressure and stored in a closed container until use. Transitions at about 60 and 65 °C were observed.

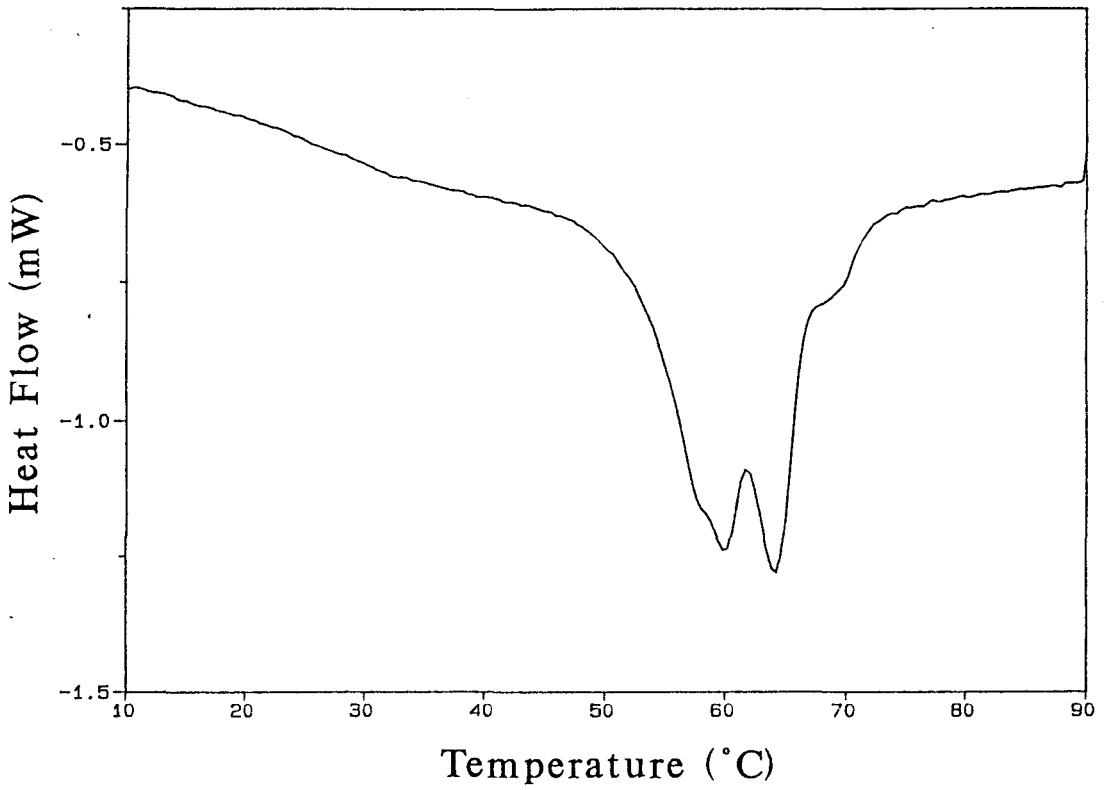
Heat Flow (mW)
-0.5
-1.0
-1.5
10
20
30
40
50
60
70
80
90
Temperature (°C)

Phase transitions for stratum corneum are complex and have been studied by X-ray diffraction, infrared spectroscopy and DSC techniques. DSC results reported transitions at 35, 65, and 80 °C for intact human stratum corneum and at 60 and 70 °C for porcine stratum corneum (Golden et al., 1986 and 1987). DSC studies of lipid extracts show a broad lipid transition at 60 °C for porcine stratum corneum (Golden et al., 1987) and at 65 °C for human stratum corneum (Golden et al., 1986). These transitions have been attributed to alkyl chain melting. Our results were in good agreement with published results.

## 3.4 Dynamic Properties of Lipids in LUVs

The EPR spectra of LUVs labeled with 5-DSA or 12-DSA at pH 9 showed a composite spectra of weakly and strongly immobilized components at all temperatures. Typical spectra of 5-DSA and 12-DSA in LUVs at 25 and 90 °C are shown in Fig. 6. As indicated in the Materials and Method section, the weakly immobilized component spectra of either 5-DSA or 12-DSA labeled LUV samples at a specific temperature were identical to spectra of 5-DSA or 12-DSA, respectively, in buffer at the same temperature. At 25 °C, the rotational correlation time obtained from the spectrum of the spin label in aqueous environment was approximately $1.3 \times 10^{-10}$ s for 5-DSA and $1.5 \times 10^{-10}$ s for 12-DSA. At 90 °C, the apparent correlation time was $3.8 \times 10^{-11}$ s for 5-DSA and $3.7 \times 10^{-11}$ s for 12-DSA. These rotational correlation time results were in good agreement with published values for doxylstearic acid spin labels dispersed in buffer (Brown et al., 1981). Thus these spectra provided evidence that the fatty acid derivative spin labels partitioned into the aqueous phase as well as into the lipid phase in LUVs.

Figure 6 **Selected EPR Spectra of 5-DSA and 12-DSA in LUVs in Fisher Borate Buffer at pH 9.** A lipid-to-spin label molar ratio of 150 with a spin label concentration of $7.5 \times 10^{-5}$ M was used. Different spin label partitions in the LUV bilayer and aqueous phases to give different intensities of broad (lipid-like) and sharp (aqueous-like) signals seen in these spectra at 25 and 90 °C.

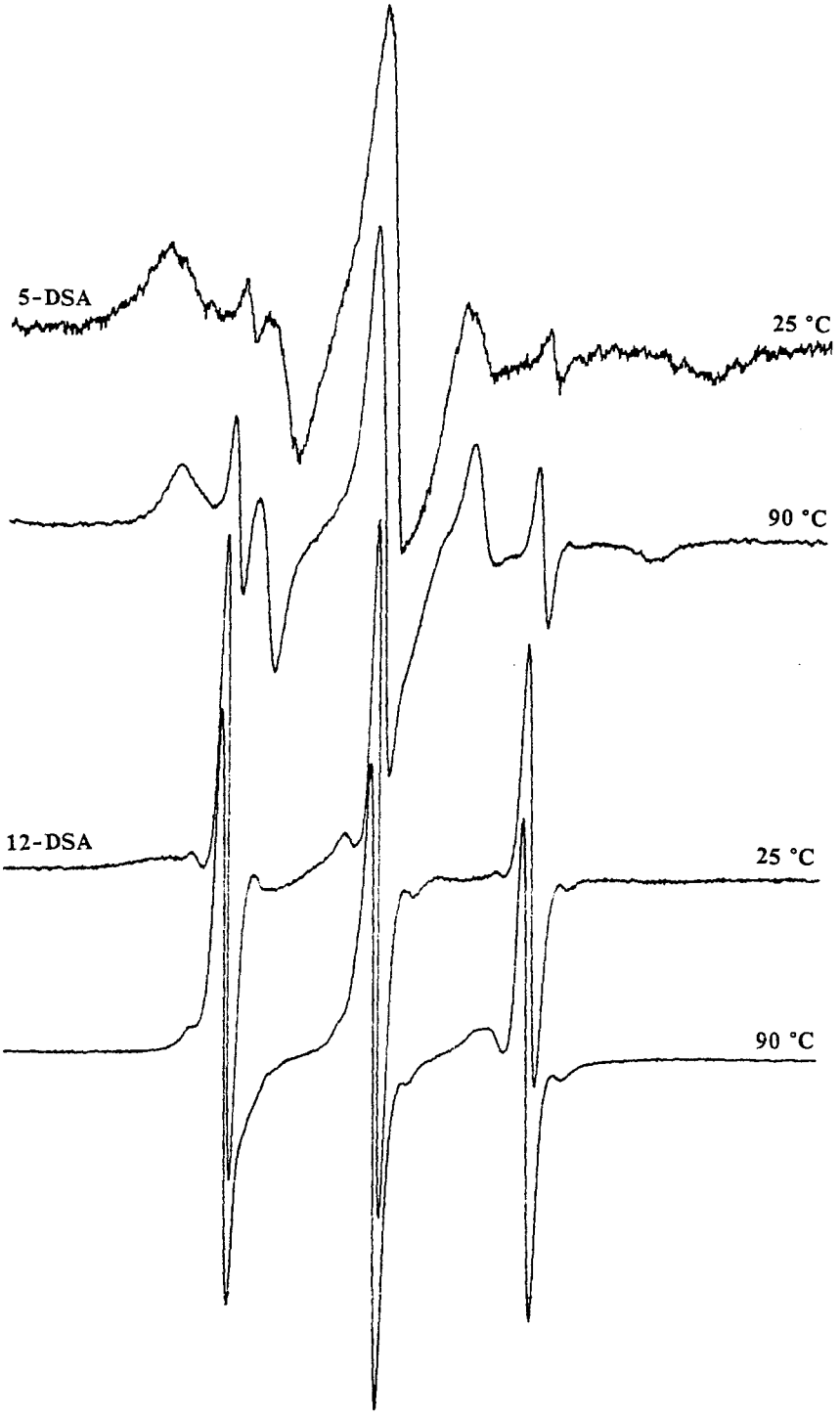
5-DSA
25 °C
90 °C
12-DSA
25 °C
90 °C

The strongly immobilized EPR signals were those of 5-DSA and 12-DSA intercalated into the lipid bilayer producing relatively slow motion. A typical spectrum, from spectral subtraction, of the strongly immobilized (lipid) component of 5-DSA in LUVs at 77 °C is shown in Fig. 1C. $2A_{max}$ of the lipid component is proportional to label mobility (Griffith et al., 1974). $2A_{max}$ has been used as an empirical measure of mobility of lipid molecules (Marsh, 1982). The $2A_{max}$ of strongly immobilized 5-DSA signals in LUVs at 25 °C was 55.4 ± 1.1 G (n = 3). The corresponding apparent rotational correlation time was about $1.2 \times 10^{-8}$ s. The $2A_{max}$ of 12-DSA in LUVs at 25 °C was 54.1 ± 3.3 G, with a corresponding apparent rotational correlation time of about $9.8 \times 10^{-9}$ s. As the temperature of the samples increased, $2A_{max}$ decreased, as expected, for both fatty acid spin labels. However, the quantitative effects of temperature on $2A_{max}$ were different for the two probes. The $2A_{max}$ values of 12-DSA (Fig. 7B) decrease much faster than those of 5-DSA (Fig. 7A) upon temperature increase. At 90 °C, $2A_{max}$ was 48.9 ± 0.6 G for 5-DSA, corresponding to a rotational correlation time of about $5.1 \times 10^{-9}$ s, but was 34.2 ± 1.1 G for 12-DSA, corresponding to ~$1.2 \times 10^{-9}$ s. For 5-DSA, $2A_{max}$ was inversely proportional to temperature, and exhibited a rather linear behavior between 25 and 90 °C. However, for 12-DSA, a gradual, but not linear, decrease in $2A_{max}$ was observed from 25 to 72 °C. The largest change in $2A_{max}$ was observed around 60 °C. Above 72 °C, little change was observed in $2A_{max}$.

## 3.5 Partitioning of Fatty Acid Spin Labels in LUVs

Since we have demonstrated that both 5-DSA and 12-DSA molecules partition between lipid and aqueous phases, the intensity ratios of the spin labels in the lipid and in

Figure 7 **Plot of the Hyperfine Splitting of the Strongly Immobilized Component ($2A_{max}$) from the Spectra of (A) 5-DSA (n = 3) and (B) 12-DSA (n = 2) in LUVs in Fisher Borate Buffer at pH 9 Versus Temperature.** A lipid-to-spin label molar ratio of 150 with a lipid concentration of 5 mg/ml was used. Note: vertical scales for the two plots differ since the two spin labels exhibit different $2A_{max}$ values. The temperature values given on the top of the plots are round off values and are not necessarily precise. Data are presented using the bottom inverse temperature scale.

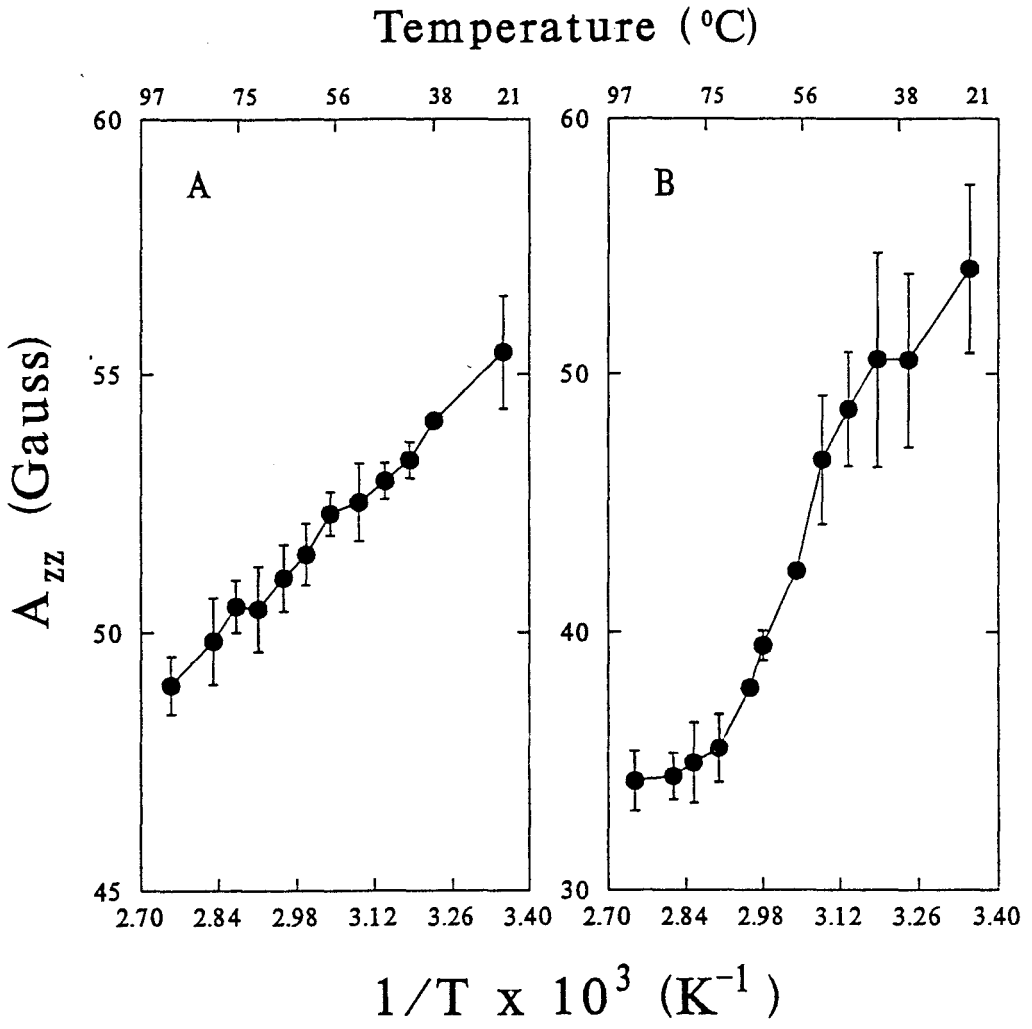
Temperature (°C)
97
75
56
38
21
A
B
$A_{zz}$ (Gauss)
60
55
50
45
40
30
2.70
2.84
2.98
3.12
3.26
3.40
1/T x $10^3$ ($K^{-1}$)

the aqueous phases provided quantitative information on the partitioning in stratum corneum LUVs. When 5-DSA and 12-DSA were introduced to LUVs at pH 9 and 25 °C at a lipid-to-spin label ratio of 150, only about 1.0 ± 0.1 % (n=3) of 5-DSA but about 26.0 ± 5.8 % (n = 2) of 12-DSA were in the aqueous phase. At 90 °C, about 4.5 ± 1.2 % of 5-DSA and about 26.3 ± 7.2 % of 12-DSA were in the aqueous phase. The partition ratio ($f_{LIPID}/f_{AQUEOUS}$) was then 96.1 ± 3.8 for 5-DSA, and only 2.9 ± 0.9 for 12-DSA at 25 °C. At 90 °C, the ratio decreased to 22.6 ± 5.7 for 5-DSA, whereas the ratio appeared to remain constant for 12-DSA (3.0 ± 1.1).

A careful study of the ratios as a function of temperature revealed interesting results. As shown in Fig. 8A, the average partition ratio ($f_{LIPID}/f_{AQUEOUS}$) for 5-DSA decreased sharply, from ~96 at 25 °C to ~42 at 37 °C and then to ~38 at 41 °C. The ratio changed only slightly from 41 to 50 °C, to a value of ~35 at 50 °C. Further increase in temperature in the range of 55 - 70 °C resulted in little change in the ratio values. Above 70 °C, the average ratio appeared to show a linear relationship with inverse temperature, resulting in a $f_{LIPID}/f_{AQUEOUS}$ of ~23 at 90 °C.

The partition ratio versus temperature plot for 12-DSA (Fig. 8B) was quite different from that of 5-DSA in the same LUV system at pH 9. The partition ratios decreased slightly as the temperature was increased from 25 to 40 °C and reached a minimum value of ~2 at 40 - 45 °C. Further increase in temperature resulted in slight increase in the partition ratio to ~3 at 70 °C. The ratio remained constant as the temperature was further increased to 90 °C. The results presented in Fig. 8B were average values of two runs. The ratios of one run were consistently higher (3.5 at 25 °C, for example) than those in the other run (2.3 at 25 °C), by

Figure 8 **Plot of the Average Partition Ratio ($f_{LIPID}/f_{AQUEOUS}$)) of (A) 5-DSA (n = 3) and (B) 12-DSA (n = 2) in LUVs in Fisher Borate Buffer at pH 9 as a Function of Temperature.** $f_{LIPID}$ values were determined from the strongly immobilized component and $f_{AQUEOUS}$ values from the weakly immobilized component. A lipid-to-spin label molar ratio of 150 with lipid concentration of 5 mg/ml was used. Spin label intensity calibration curves was used to determine spin label intensities at different temperatures. Such procedures were required to account for the different EPR cavity sensitivity at different temperatures. Note: Vertical scales for the two plots are different due to large differences in partition values of the two spin labels. The temperature values given on the top of the plots are round off values and are not necessarily precise. Data are presented using the bottom inverse temperature scale.

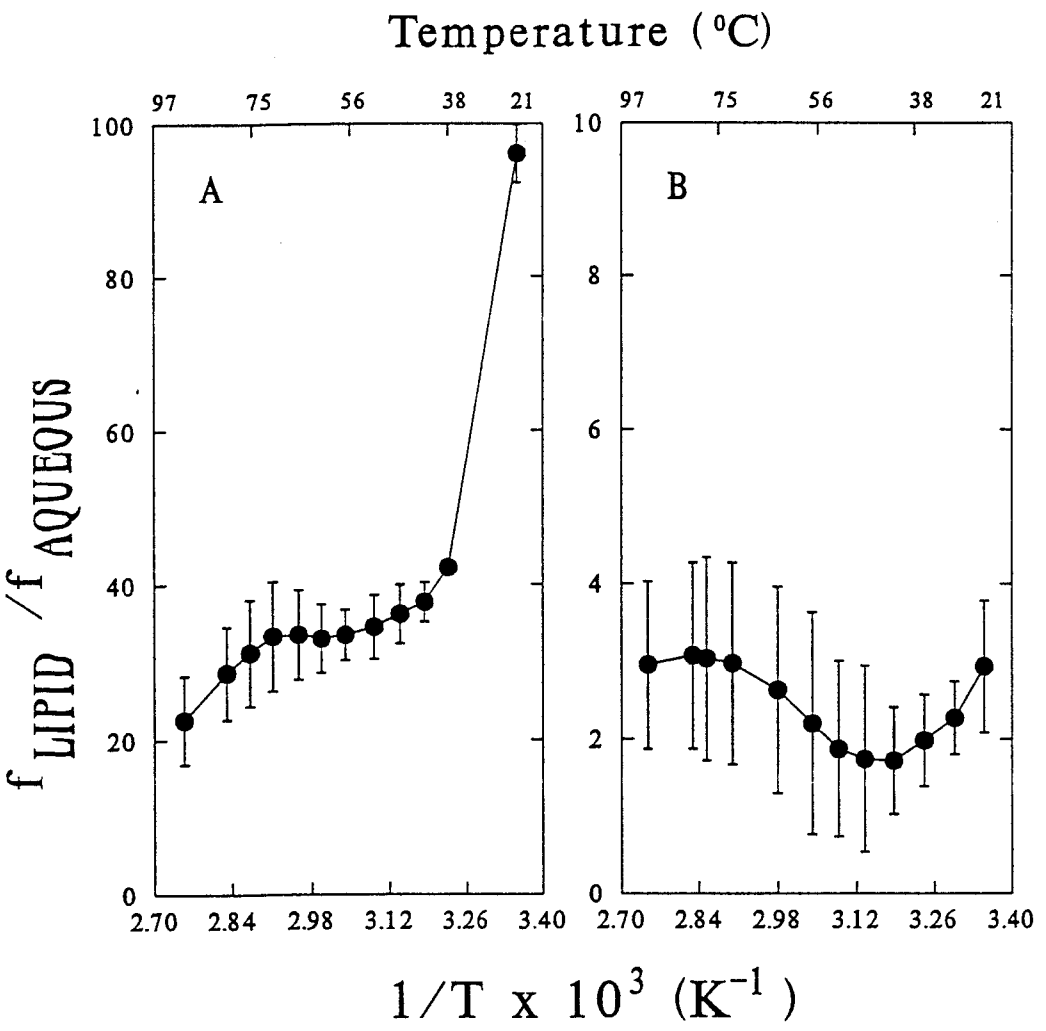
Temperature (°C)
97
75
56
38
21
A
B
100
80
60
40
20
0
10
8
6
4
2
0
2.70
2.84
2.98
3.12
3.26
3.40
f LIPID / f AQUEOUS
1/T x 10^3 (K^-1)

about a constant amount throughout the temperature range studied, with the minimum around 40 - 45 °C (2.2 for the run with higher values and 0.9 for the run with lower values). Thus, the temperature-induced changes in the partition coefficients for 12-DSA in LUVs were very reproducible from run to run, despite the magnitudes of the changes being quite small (maximum changes were about 1.5).

## 3.6 Effect of Salt on Effective Diameter of SC LUVs

LUVs (5 mg/ml) prepared in Fisher borate buffer without fluorescence probes have an effective diameter of 119 ± 10 nm (n = 16 preparations) and a polydispersity of 0.086 ± 0.019 (See page 35). The addition of ANTS and/or DPX results in an increase in osmolality. Therefore, KCl (~60 mM) was added to Fisher borate buffer in the preparation of LUVs to simulate the salt effect when ANTS and DPX were encapsulated in LUVs. The effective diameter of the LUVs with increased salt was 124 ± 9 nm (n = 2) with a polydispersity of 0.114 ± 0.019. Thus, increasing the salt concentration of the LUVs does not change the effective diameter of the LUVs.

## 3.7 Effect of Fluorescent Probe Concentration on SC LUV Diameter

The effect of probe concentration on the effective diameter and polydispersity of LUVs is shown in Table 4. When normal SC LUVs were encapsulated with 12.5 or 25 mM ANTS, little change in effective diameter and polydispersity was observed (i.e. 128 ± 16 nm with a polydispersity of 0.120 ± 0.054 and 120 ± 7 nm with a polydispersity of 0.114 ± 0.029, respectively). These values also agree well with empty SC LUVs prepared in borate buffer.

Table 4 Effect of Fluorescent Probe Concentration on Normal SC LUVs

| Encapsulated Probe | Probe Conc. (mM) | ED[a] (*n*) | PD[b] (*n*) |
|---|---|---|---|
| ANTS | 50 | 170 (1) | 0.209 (1) |
| ANTS | 25 | 120 ± 7 (3) | 0.114 ± 0.029 (3) |
| ANTS | 12.5 | 128 ± 16 (2) | 0.120 ± 0.054 (2) |
| DPX | 50 | 121 ± 14 (2) | 0.145 ± 0.008 (2) |
| DPX | 25 | 138 (1) | 0.163 (1) |

[a]ED is the effective diameter in nanometers of LUVs ± the standard deviation (*n*, number of different samples used).

[b]PD is the polydispersity (the relative width of the distribution).

Thus, encapsulating SC LUVs with ANTS at concentrations less than 25 mM does not effect the diameter or the distribution of diameters in LUVs. However, encapsulating 50 mM ANTS in normal SC LUVs resulted in an increase in effective diameter (170 nm) and polydispersity (0.209). The encapsulation of DPX in normal SC LUVs was more difficult to achieve than ANTS encapsulation. In general, more than 10 extrusions through 0.1 μm filters were required to prepare LUVs. The effective diameter (polydispersity) obtained for SC LUVs encapsulated with 25 mM DPX was 138 nm (0.163) and with 50 mM DPX was 121 ± 14 nm (0.145 ± 0.008). However, when 90 mM DPX was present in the encapsulation buffer, vesicles could not be formed. This is in contrast to phosphatidylserine (PS) LUVs which can be prepared with 90 mM DPX encapsulated (Ellens et al., 1985). Thus for our fusion experiments, we chose to encapsulate 12.5 mM ANTS and 25 mM DPX in different compositions of SC LUVs for leakage studies. Additionally, 25 mM ANTS SC LUVs and 50 mM DPX SC LUVs were used for contents mixing studies in order to reduce the effect of high probe concentrations on LUV size and size distribution.

## 3.8 Binding of ANTS to LUVs

The fluorescence intensity of normal SC LUVs incubated with 25 mM ANTS and then column separated was <1 % of the total fluorescence intensity of LUVs encapsulated with ANTS. In addition, the effective diameter of the LUVs did not significantly change after incubation with ANTS (131 versus 135 nm in a paired run). The fluorescence intensity of DPPC LUVs incubated with ANTS and then column separated was also < 1 % of the total fluorescence intensity of ANTS encapsulated in LUVs. Also, the effective diameter of the

LUVs did not change after incubation with ANTS (86 nm). These results are similar to the results obtained from empty PS LUVs incubated with 12.5 mM ANTS (Ellens et al., 1985). Thus, 25 mM ANTS does not significantly interact with SC lipid bilayers and remains in the aqueous phase inside the vesicles.

## 3.9 Lipid Composition of ANTS SC LUVs

HPTLC analysis of LUV lipids from all three lipid compositions used in this study are shown in Fig. 9. The lipids were extracted from samples containing 25 mM ANTS. Also shown are lipid standards used to help identify lipids (lane 4). By inspection, as the lipid composition of LUVs changes from 0 % cholesterol sulfate ($ChSO_4$) and 30 % cholesterol (lane 1) to 5 % cholesterol sulfate and 25 % cholesterol (lane 2) and to 15 % cholesterol sulfate and 15 % cholesterol (lane 3), the intensities of the spots on the HPTLC plate due to cholesterol sulfate increased while the intensities of the spots due to cholesterol decreased. Furthermore, the spots due to the other lipids remained essentially the same. Thus, after extrusion and column separation, the lipid compositions of the ANTS LUVs were similar to their starting compositions before extrusion (Table 1).

## 3.10 Lipid Concentration and QELS Results of SC LUVs Used for Fluorescence Studies

Since the lipid compositions of the dilute SC LUVs were similar to the lipid composition of the starting materials, the cholesterol concentration of each dilute sample was used to calculate the concentration of total lipid. The lipid concentration of LUVs with the different lipid compositions used for leakage and contents mixing assays are shown in Table

Figure 9 **High Performance Thin Layer Chromatogram of the Lipids from Various Composition SC LUVs Encapsulated with 25 mM ANTS.** The identities of individual lipids are shown on the right. Lane assignments are as follows: lane 1- 0 % $ChSO_4$ SC LUVs, lane 2- 5% $ChSO_4$ SC LUVs, lane 3- 15 %$ChSO_4$ SC LUVs, lane 4- lipid standards with each lipid at a concentration of 1mg/ml. About 20 μg total lipid were applied to lanes 1 - 3 and 35 μg total lipid to lane 4.

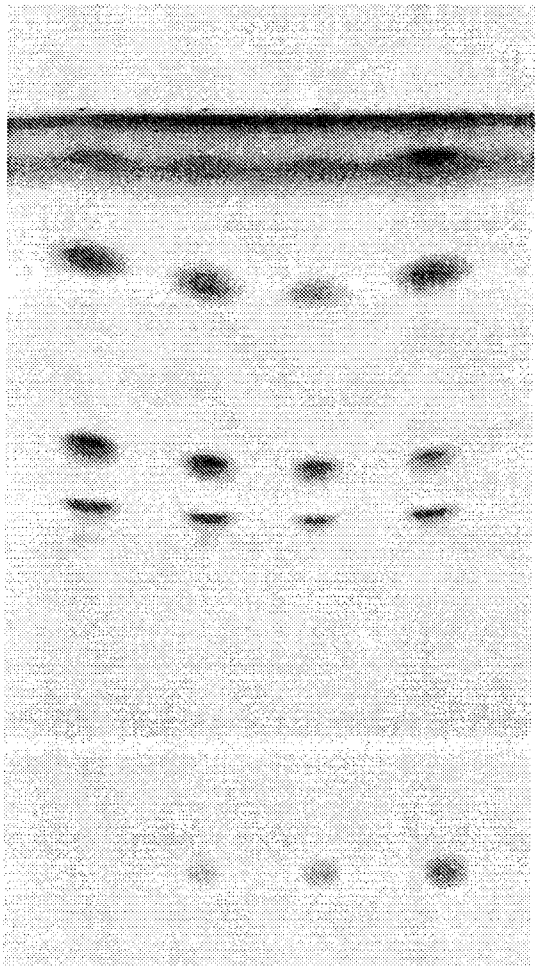

fatty acids

cholesterol

ceramide type III

ceramide type IV

cholesterol sulfate

1 2 3 4

Table 5 QELS Particle Size Analysis and Total Lipid Concentration of Probe Encapsulated LUVs at pH 9 Used for Leakage and Contents Mixing Assays

| Encapsulated Probes | % Cholesterol sulfate | ED[a] (*n*) | PD[b] (*n*) | [Lipid][c] (*n*) |
|---|---|---|---|---|
| 25 mM ANTS | 0 | 119 ± 35 (2) | 0.164 ± 0.064 (2) | 1.05 ± 0.36 (3) |
| 50 mM DPX | 0 | 154 ± 16 (3) | 0.181 ± 0.076 (3) | 0.73 ± 0.46 (3) |
| 12.5 mM ANTS/ 25 mM DPX | 0 | 124 ± 9 (3) | 0.118 ± 0.043 (3) | 0.83 ± 0.13 (3) |
| 25 mM ANTS | 5 | 116 ± 3 (2) | 0.100 ± 0.022 (2) | 1.30 ± 0.23 (2) |
| 50 mM DPX | 5 | 121 ± 14 (2) | 0.145 ± 0.008 (2) | 0.86 ± 0 (2) |
| 12.5 mM ANTS/ 25 mM DPX | 5 | 117 ± 20 (3) | 0.102 ± 0.048 (3) | 1.30 ± 0.29 (3) |
| 25 mM ANTS | 15 | 105 ± 9 (2) | 0.088 ± 0.008 (2) | 1.45 ± 0.06 (2) |
| 50 mM DPX | 15 | 121 ± 7 (2) | 0.137 ± 0.064 (2) | 1.14 ± 0.10 (2) |
| 12.5 mM ANTS/ 25 mM DPX | 15 | 111 ± 6 (4) | 0.102 ± 0.035 (4) | 1.03 ± 0.23 (4) |
| Average | 0-15 | 121 ± 14 (23) | 0.126 ± 0.032 (23) | 1.03 ± 0.35 (24) |

[a]ED is the average effective diameter in nanometers of LUVs ± the standard deviation (*n*, number of different samples used).

[b]PD is the polydispersity (the relative width of the distribution of ED).

[c][Lipid] represents the concentration of total lipid in mg/ml of probe containing LUVs after column separation. The total lipid concentration is computed by assuming that the cholesterol concentration (determined via the cholesterol oxidase assay) represents the concentration of total lipid.

5 (last column). The average, mean lipid concentration amongst all of the different compositions was 1.03 ± 0.35 mg/ml with a range between 0.73 and 1.45 mg/ml.

LUVs used in leakage and contents mixing experiments were also characterized by QELS. The average effective diameters (polydispersities) of LUVs prepared with 5 and 15 % cholesterol sulfate ranged from 105 ± 9 nm (0.088 ± 0.008) to 121 ± 14 nm (0.145 ± 0.008). In general, the average polydispersity values were slightly higher with 50 mM DPX encapsulation than with 25 mM ANTS encapsulation for these two lipid compositions (i.e. 0.100 and 0.088 versus 0.145 and 0.137, respectively), indicating that the DPX LUVs had a broader distribution of effective diameters than the ANTS LUVs. For the LUVs prepared with 0% cholesterol sulfate, ANTS (25 mM) encapsulation resulted in LUVs with average effective diameters of 119 ± 35 nm, similar to those obtained for the other lipid compositions. However, DPX (50 mM) LUVs containing 0% cholesterol sulfate were much more difficult to prepare and exhibited an average effective diameter of 154 ± 16 nm with an average polydispersity of 0.181 ± 0.076. Thus, LUVs encapsulated with DPX were generally larger than those encapsulated with ANTS, and the distributions of diameters were broader. Moreover, the inclusion of cholesterol sulfate in the lipid composition partially reduced the size increase observed with DPX encapsulation.

## 3.11 Quenching of ANTS Fluorescence by DPX in DPPC and SC LUVs

Since different concentrations of ANTS and DPX were used for leakage and contents mixing assays with SC LUVs in comparison to published work with phospholipid vesicles (Ellens et al., 1984 and 1985), it was necessary to determine the extent of quenching in SC

LUVs under ANTS and DPX concentrations used in our studies. DPPC LUVs were also tested for comparison with our samples as well as with published phospholipid vesicle data. The degrees of quenching (% $F_{max}$) of 12.5 mM ANTS by 12.5, 25 and 50 mM DPX in normal SC LUVs and DPPC LUVs are shown in Fig. 10. Both types of LUVs displayed similar quenching profiles. As the DPX concentration in LUVs was increased from 12.5 to 25 mM, the % of ANTS fluorescence quenched by DPX increased from approximately 65 % to 80 %. Moreover, as the concentration of DPX was increased to 45 mM, the ANTS fluorescence was approximately 90 % quenched. From these quenching profiles, we demonstrated that ANTS was significantly quenched by DPX at the concentrations used in our experiments.

## 3.12 Curve Fitting of Leakage and Aqueous Contents Mixing Data

The leakage and aqueous contents mixing fluorescence data was fitted to one of three equations described in the data analysis section of Materials and Methods. An example of data reproducibility and curve fitting for a leakage experiment is shown in Fig. 11. The particular example chosen is 5 mM $Ca^{2+}$-induced leakage of normal lipid composition SC LUVs. The % maximum fluorescence from three separate experiments (shown as three different open symbols) is plotted as a function of time. The dotted line through each set of symbols represents the best fit through the data points. Average values (stars) from the fitted lines are also shown. For the example chosen, the data was fitted to the four-parameter double exponential equation previously described. As shown in Fig. 11, the line goes through most of the data points indicating that the data averaging method that we used (Section 2.19)

Figure 10 **The Quenching of 12.5 mM ANTS by 12.5, 25 and 50 mM DPX in Normal SC LUVs and DPPC LUVs.** Plotted is the % max fluorescence of the sample that is quenched as a function of DPX concentration. The closed square symbols represent SC LUVs and the open circle symbols represent DPPC LUVs.

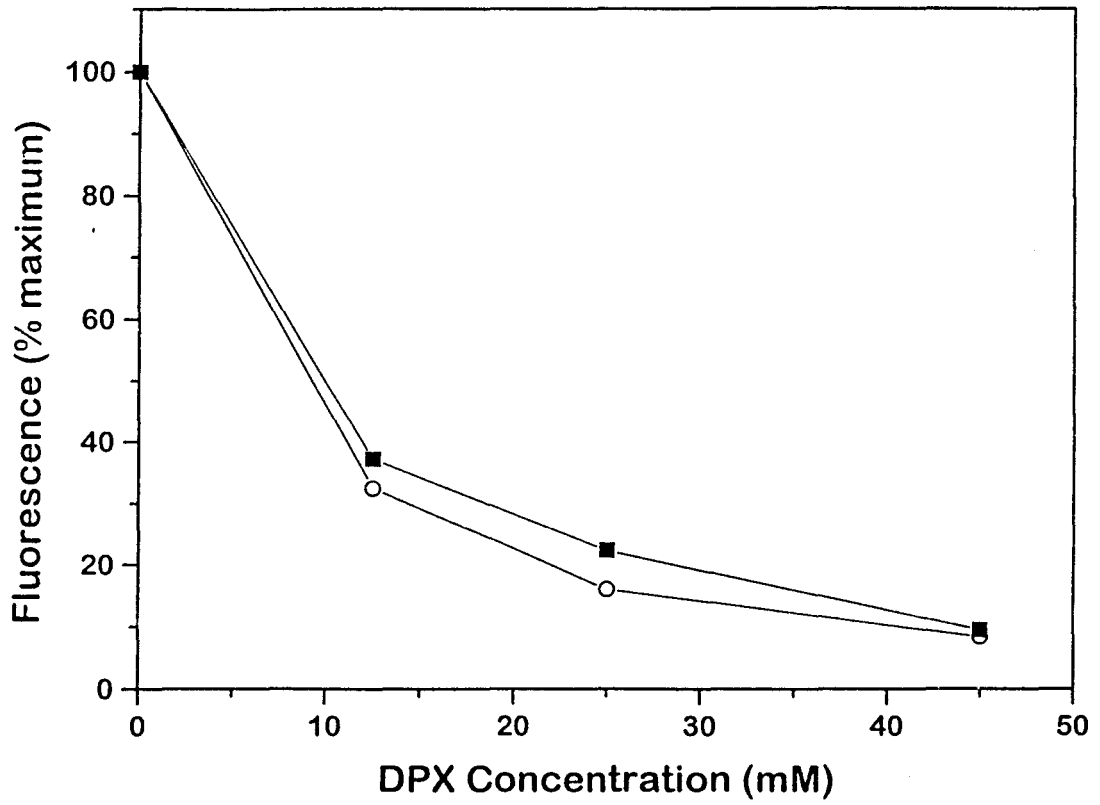
Fluorescence (% maximum)
100
80
60
40
20
0
0
10
20
30
40
50
DPX Concentration (mM)

Figure 11 **An Example of the Variation in Experimental Data and Curve Fitting for 5 mM $Ca^{2+}$-Induced Leakage of Normal SC LUVs.** The three different open symbols (squares, triangles, and circles) represent three separate runs of data from different LUV preparations. The dotted line through each curve represents the best fit through the points. The closed star symbols represent average values from the three fitted lines.

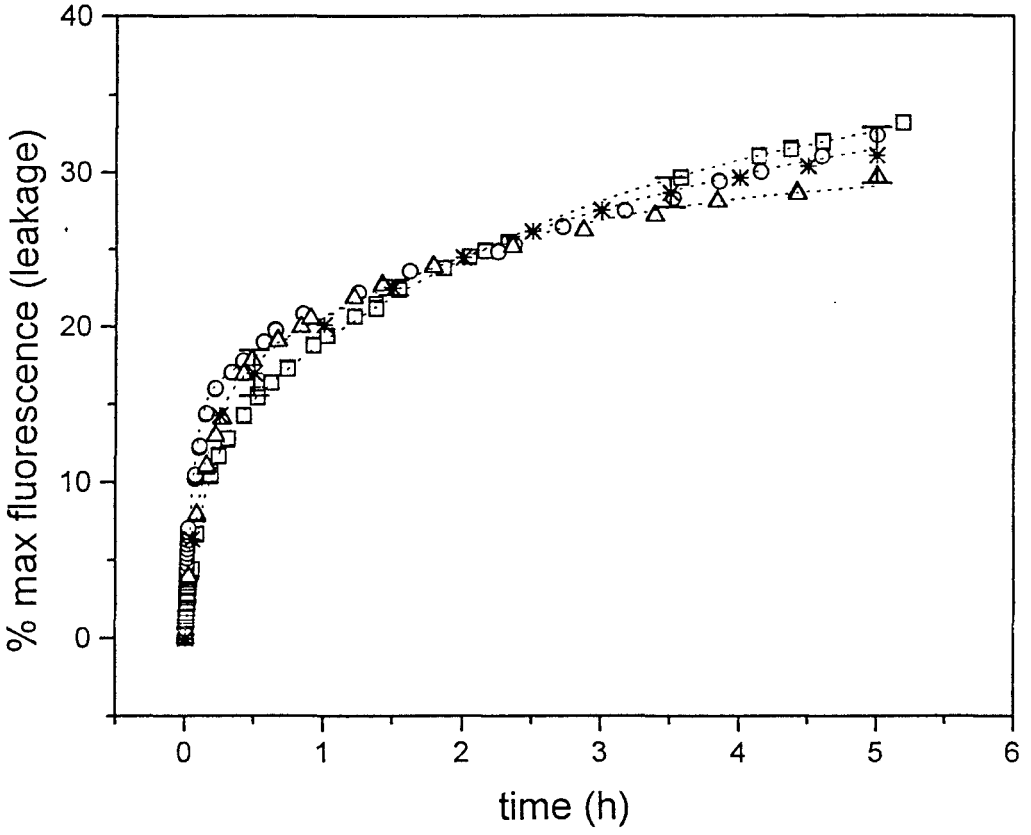
% max fluorescence (leakage)
time (h)
0
10
20
30
40
0
1
2
3
4
5
6

is valid.

### 3.13 Stability of ANTS/DPX LUVs at pH 9

The results of leakage and contents mixing assays of various lipid composition SC LUVs at pH 9 are shown in Figs. 12 and 13, respectively. These results suggest that leakage of all SC LUVs (Fig. 12), regardless of lipid composition, is extremely small over 5 hours, indicating that these LUVs are quite stable at pH 9. In contrast, a slight increase in the average aqueous contents mixing of the LUVs was observed over 5 h for all lipid compositions used (Fig. 13). After 5 h, the average contents mixing increased to about 2, 4, and 5 % for 15, 5 and 0 % cholesterol sulfate-containing LUVs, respectively.

### 3.14 Stability of ANTS/DPX LUVs at pH 6

#### 3.14.1 Effect of Different Lipid Compositions on Leakage at pH 6

The leakage of SC LUVs as a result of dialysis to pH 6 is shown in Fig. 14. For 5 and 15 % cholesterol sulfate-containing LUVs, the pH-induced leakage was similar. LUVs containing 5 % cholesterol sulfate exhibited about 10 % leakage in the first hour and leveled off at about 15 % leakage at 5 hours. LUVs containing 15 % cholesterol sulfate exhibited a similar leakage profile but with slightly reduced levels of leakage; about 7 % leakage was observed at t = 1 h and about 10 % at t = 5. Since errors of the measurements were relatively large, it is difficult to quantitatively determine these differences between 5 and 15 % cholesterol sulfate-containing LUVs. In contrast, the LUVs containing 0 % cholesterol sulfate exhibited a completely different pH-induced leakage profile (Fig. 14). There appeared

Figure 12 **Leakage of Various Lipid Composition SC LUVs at pH 9**. Plotted is the average fitted data of the % maximum fluorescence as a function of time for 0 % $ChSO_4$ SC LUVs (closed squares, n = 2), 5 % $ChSO_4$ SC LUVs (open circles, n = 3), and 15 % $ChSO_4$ SC LUVs (closed triangles, n = 4).

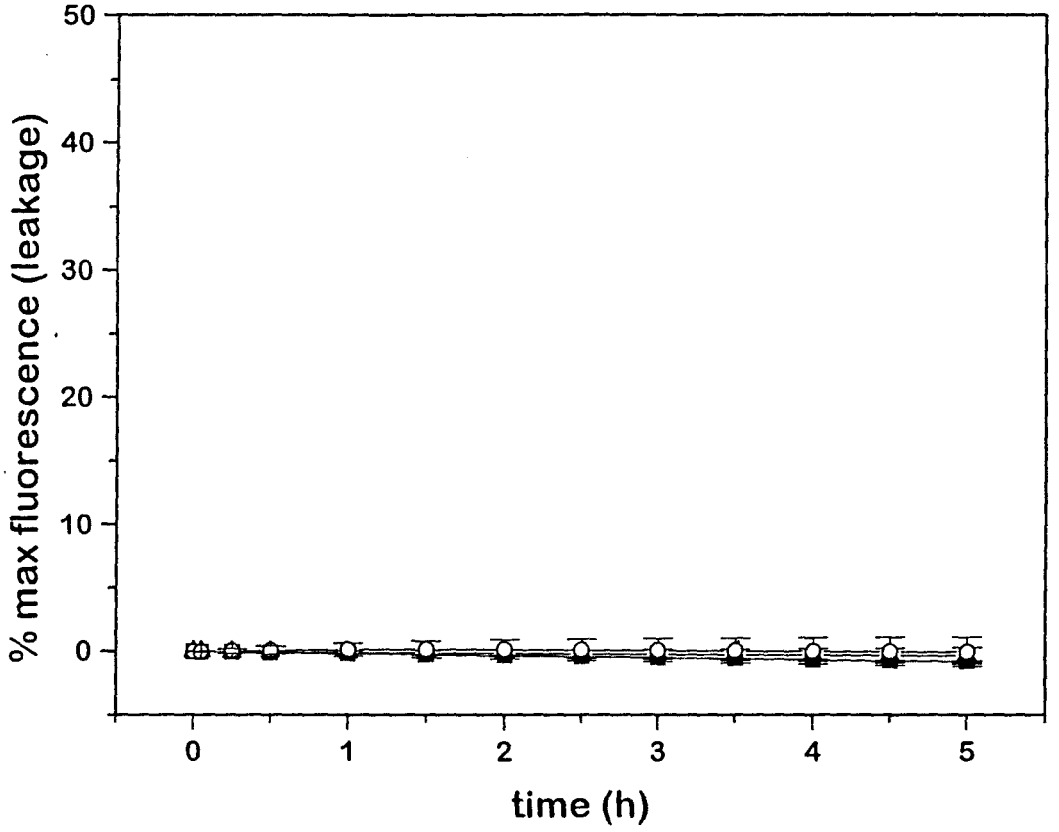
% max fluorescence (leakage)
50
40
30
20
10
0
0
1
2
3
4
5
time (h)

Figure 13 **Aqueous Contents Mixing of Various Lipid Composition SC LUVs at pH 9.** Plotted is the average fitted data of the % maximum fluorescence as a function of time for 0 % $ChSO_4$ SC LUVs (closed squares, n = 4), 5 % $ChSO_4$ SC LUVs (open circles, n = 3), and 15 % $ChSO_4$ SC LUVs (closed triangles, n = 3).

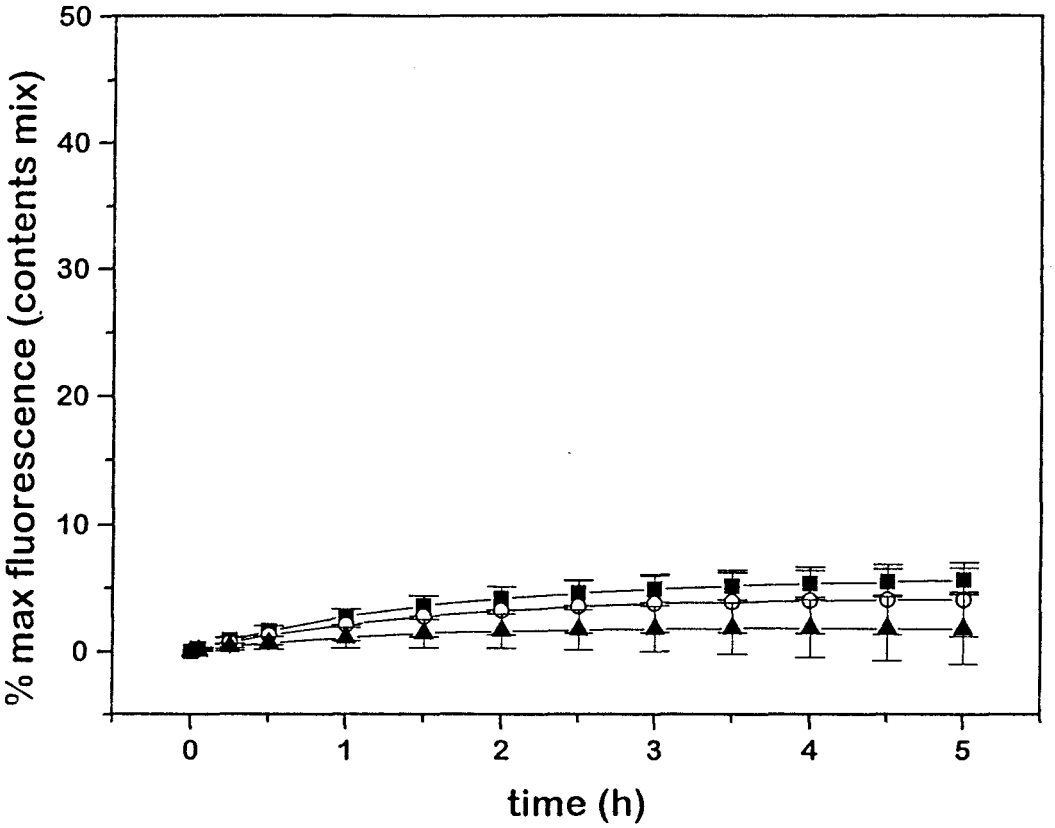
% max fluorescence (contents mix)
50
40
30
20
10
0
0
1
2
3
4
5
time (h)

Figure 14 **Leakage of Various Lipid Composition SC LUVs at pH 6.** Plotted is the average fitted data of the % maximum fluorescence as a function of time for 0 % $ChSO_4$ SC LUVs (closed squares, n = 3), 5 % $ChSO_4$ SC LUVs (open circles, n = 3), and 15 % $ChSO_4$ SC LUVs (closed triangles, n = 4).

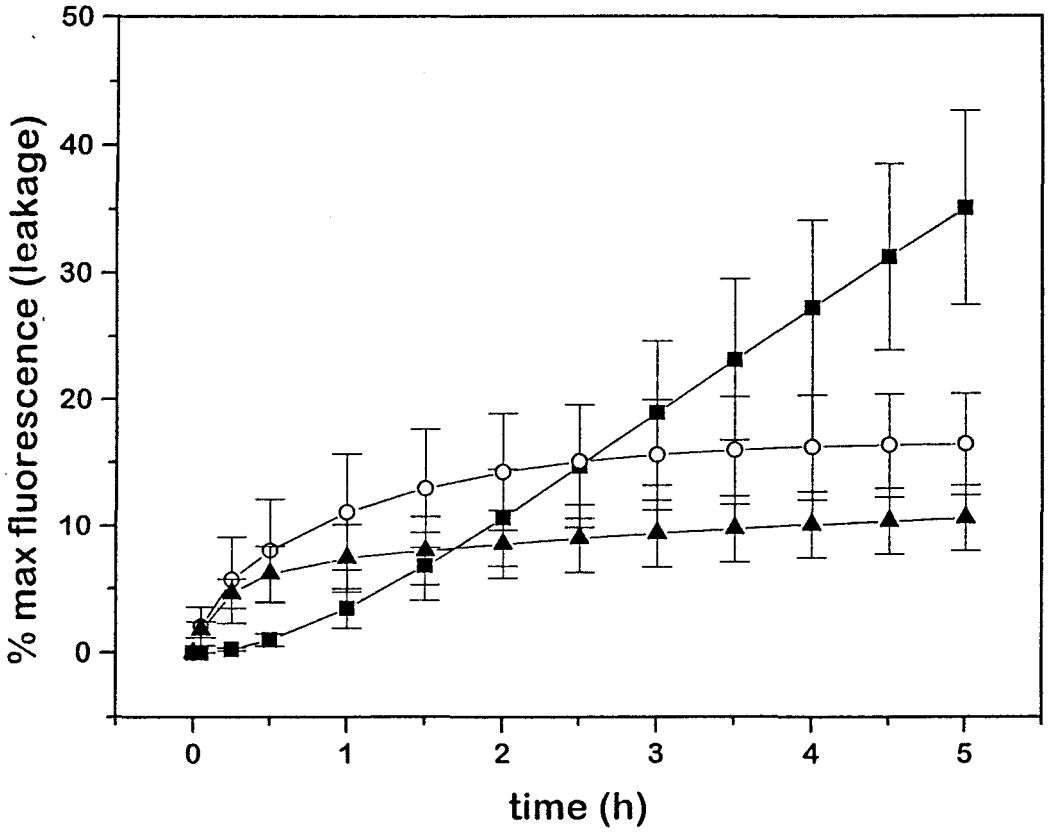
% max fluorescence (leakage)
50
40
30
20
10
0
0
1
2
3
4
5
time (h)

to be a lag phase within the first hour of measurements, where little leakage was observed. After the first hour, however, leakage increased steadily from about 2 % at t = 1 h to about 36 % at t = 5 h. Thus, after 5 h, these LUVs were considerably less stable than those with cholesterol sulfate.

### 3.14.2 Effect of Different Lipid Compositions on Aqueous Contents Mixing at pH 6

The effect of dialyzing SC LUVs from pH 9 to pH 6 on the aqueous contents mixing of the LUVs is displayed in Fig. 15. All lipid compositions showed similar contents mixing profiles. The extent of contents mixing within 5 h was greatest for 5 % cholesterol sulfate-containing LUVs (~16 %). In comparison, 0 and 15 % cholesterol sulfate-containing LUVs exhibited 12 and 9 % contents mixing, respectively, at t = 5 h. Within the error of the measurement, it is difficult to determine whether these differences are statistically significant.

### 3.14.3 Comparison of pH 6-Induced Leakage and Aqueous Contents Mixing by Dialysis or Concentrated Acid Injection for Normal SC LUVs

The pH of LUVs for leakage and contents mixing experiments was lowered by dialysis against an isosmotic buffer at pH 6. An additional set of pH-induced leakage and contents mixing experiments was performed on SC LUVs containing 5 % cholesterol sulfate. The pH in these experiments was lowered to 6.0 immediately by injection of concentrated MES acid. A comparison of the results from the dialysis and injection methods for leakage and contents mixing are shown in Figs. 16 and 17, respectively. As shown in Fig. 16, over 5 h the LUV average leakage induced by injection of MES acid slowly increased to 5 % while the average

Figure 15 **Aqueous Contents Mixing of Various Lipid Composition SC LUVs at pH 6.** Plotted is the average fitted data of the % maximum fluorescence as a function of time for 0 % $ChSO_4$ SC LUVs (closed squares, n = 3), 5 % $ChSO_4$ SC LUVs (open circles, n = 3), and 15 % $ChSO_4$ SC LUVs (closed triangles, n = 3).

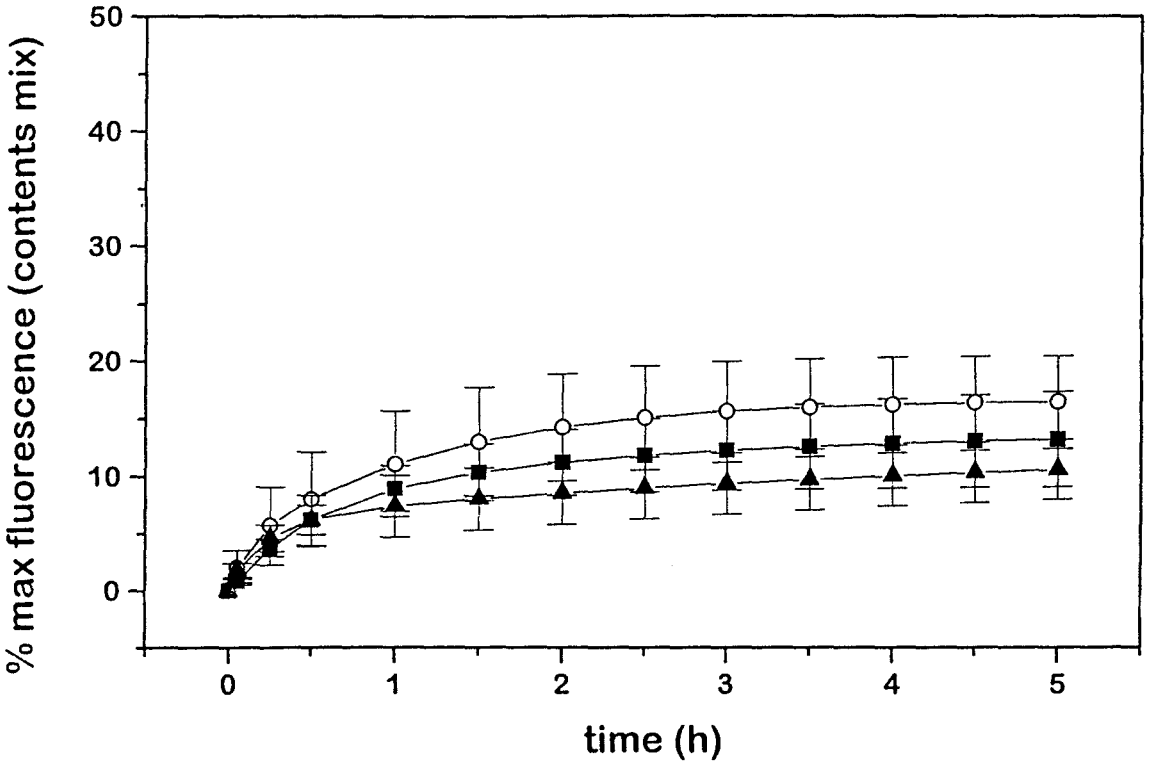
% max fluorescence (contents mix)
50
40
30
20
10
0
0
1
2
3
4
5
time (h)

Figure 16 **Comparison of pH 6-Induced Leakage of Normal SC LUVs by Dialysis and Injection Methods.** Plotted is the average fitted data of the % maximum fluorescence as a function of time for normal SC LUVs lowered from pH 9 to pH 6 by dialysis (open circles, n = 3) and by concentrated MES acid injection (closed circles, n = 2).

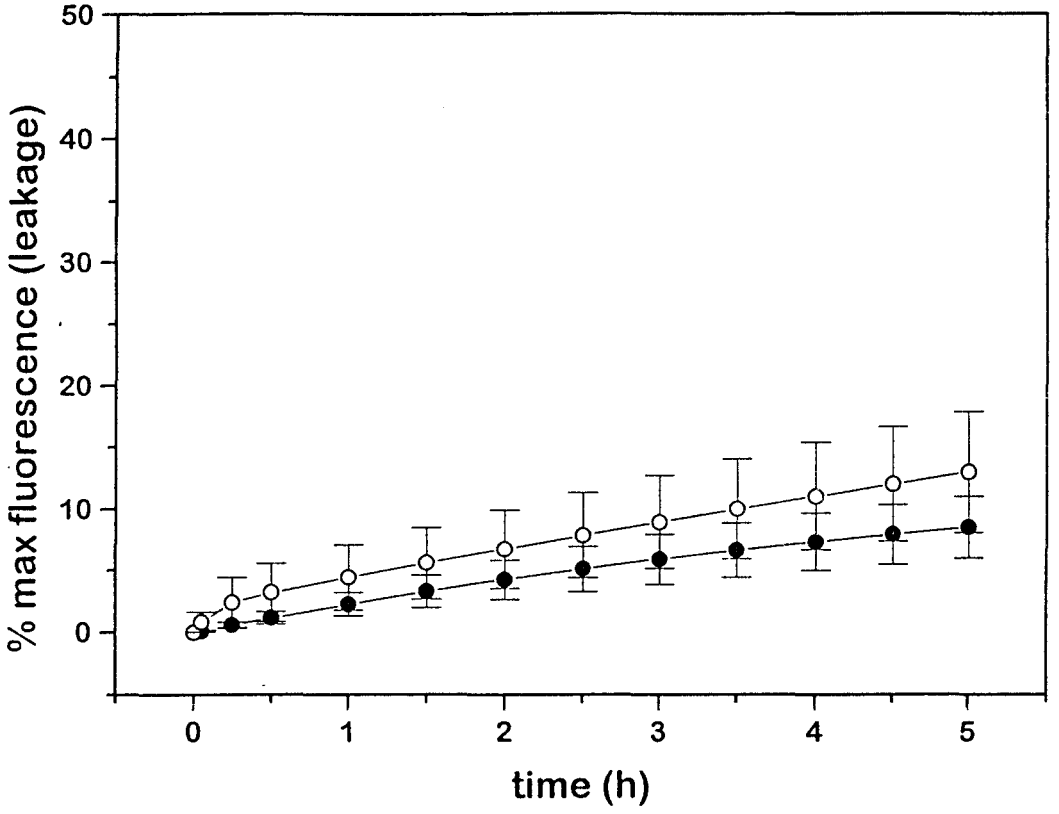
% max fluorescence (leakage)
50
40
30
20
10
0
0
1
2
3
4
5
time (h)

Figure 17 **Comparison of pH 6-Induced Aqueous Contents Mixing of Normal SC LUVs by Dialysis and Injection Methods.** Plotted is the average fitted data of the % maximum fluorescence as a function of time for normal SC LUVs lowered from pH 9 to pH 6 by dialysis (open circles, n = 3) and by concentrated MES acid injection (closed circles, n = 2).

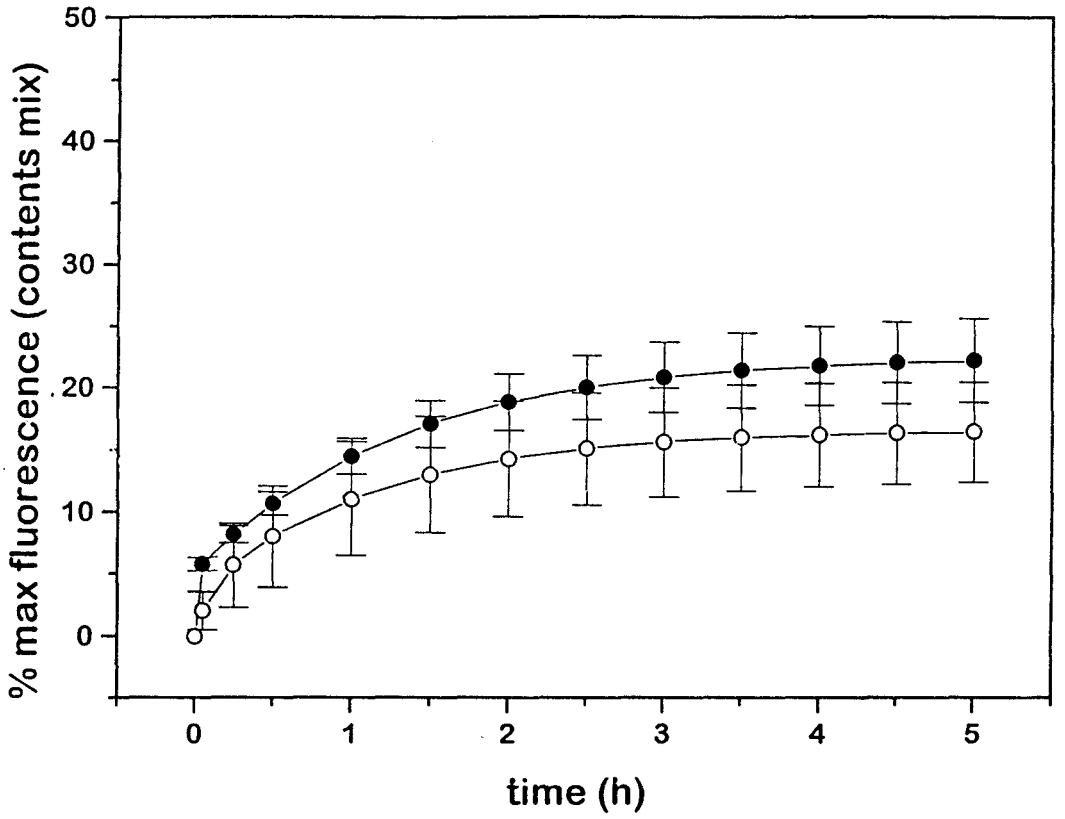
% max fluorescence (contents mix)
50
40
30
20
10
0
0
1
2
3
4
5
time (h)

leakage induced by dialysis increased to about 10 %. However, the variability within the measurements indicated that these differences might not be significant. Similarly, slight differences in results were also observed between injection and dialysis methods for pH 6-induced contents mixing (Fig. 17). About 13 % contents mixing was observed by the dialysis method, whereas 18 % was observed by the injection method. Once again , the variability between the measurements suggested that the differences might not be statistically significant.

## 3.15 Effect of Different Lipid Compositions on Leakage Induced by 5 mM $Ca^{2+}$

The effect of $Ca^{2+}$ on the leakage of SC LUVs is shown in Fig. 18. Similar leakage profiles are observed for 5 and 15 % cholesterol sulfate-containing LUVs. Leakage increased from 0 to 17 % within the first 30 min. Approximately 30 % leakage was observed for the cholesterol-sulfate containing LUVs within 5 h. In contrast, the $Ca^{2+}$-induced leakage of LUVs with 0 % cholesterol sulfate was initially slower than cholesterol sulfate- containing samples. About 13 % leakage was observed in the first 30 min. However, the leakage of the 0 % cholesterol sulfate-containing LUVs then increased sharply to about 45 % at t = 5 h.

## 3.16 Effect of Different Lipid Compositions on Contents Mixing Induced by 5 mM $Ca^{2+}$

The effects of $Ca^{2+}$ on the aqueous contents mixing of all the SC LUVs (Fig. 19) were similar, regardless of the % cholesterol sulfate present. All SC LUV compositions showed about 30 % aqueous contents mixing within the first 3 minutes of measurements. This value leveled off at about 35 % within 1 h. No further changes were observed over the next 4 h.

Figure 18 **$Ca^{2+}$-Induced Leakage of Various Lipid Composition SC LUVs at pH 9.** Plotted is the average fitted data of the % maximum fluorescence as a function of time for 0 % $ChSO_4$ SC LUVs (closed squares, n = 3), 5 % $ChSO_4$ SC LUVs (open circles, n = 3), and 15 % $ChSO_4$ SC LUVs (closed triangles, n = 4).

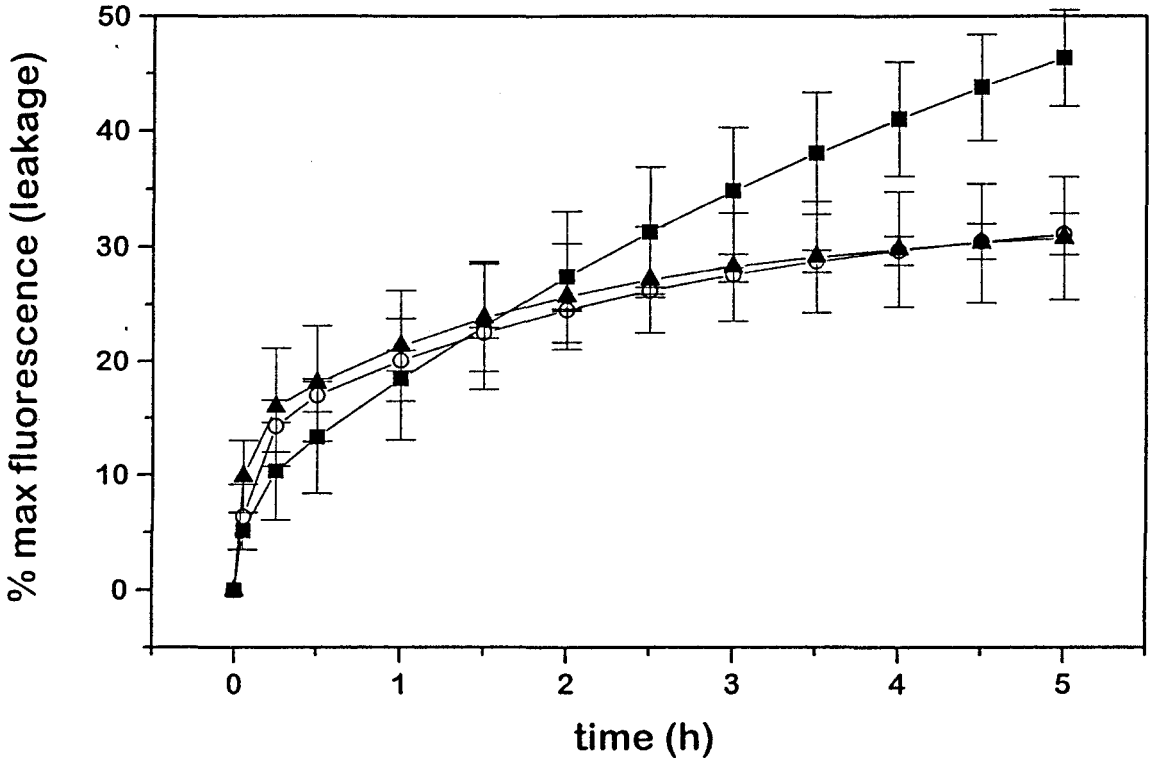
% max fluorescence (leakage)
50
40
30
20
10
0
0
1
2
3
4
5
time (h)

Figure 19 **$Ca^{2+}$-Induced Aqueous Contents Mixing of Various Lipid Composition SC LUVs at pH 9.** Plotted is the average fitted data of the % maximum fluorescence as a function of time for 0 % $ChSO_4$ SC LUVs (closed squares, n = 4), 5 % $ChSO_4$ SC LUVs (open circles, n = 3), and 15 % $ChSO_4$ SC LUVs (closed triangles, n = 3).

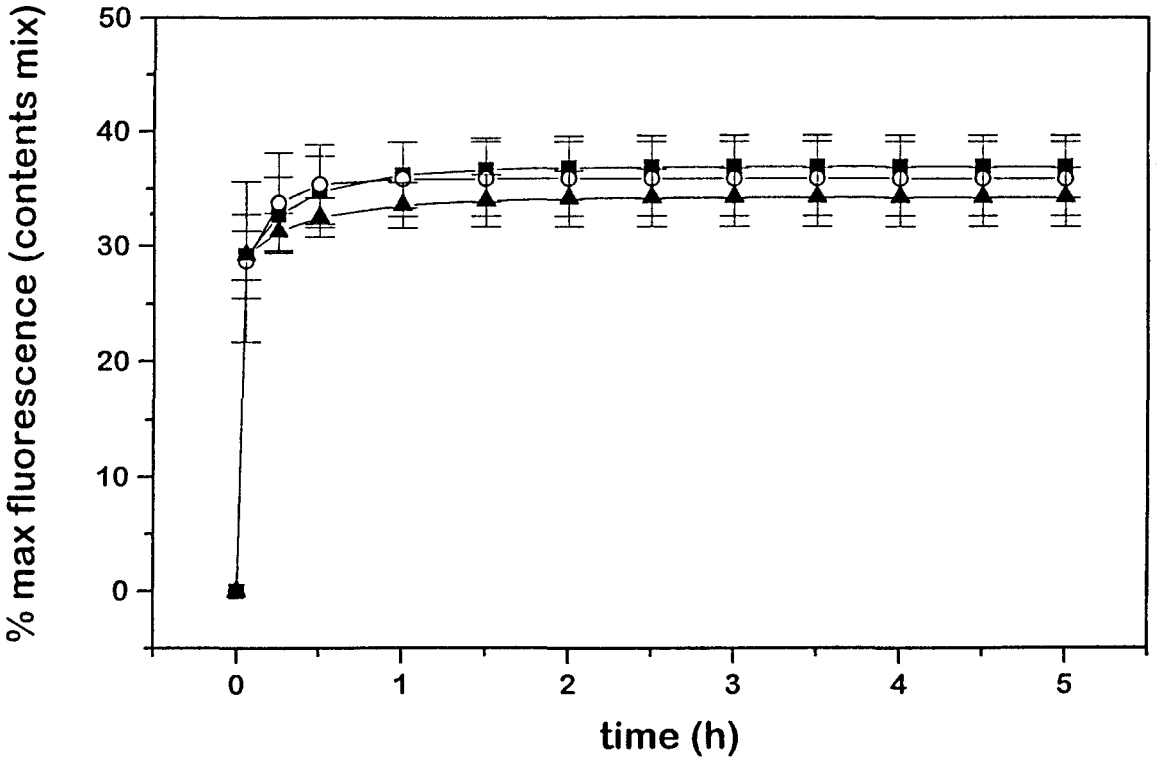
% max fluorescence (contents mix)
50
40
30
20
10
0
0
1
2
3
4
5
time (h)

# CHAPTER IV

# DISCUSSION

## 4.1 LUVs as a Model System of SC Lipids

We have described detailed procedures for using lipids that are commercially available to prepare stratum corneum LUVs at pH 9 by extrusion methods. A model system consisting of conveniently available lipid components will presumably generate more studies of the system, leading to a better understanding of stratum corneum lipids on a molecular level. The experimentally determined lipid composition in LUVs was about 33 % (by weight) ceramide III, 25 % cholesterol, 21 % ceramide IV, 16 % total free fatty acids and 5 % cholesterol sulfate, a lipid composition very similar to that of the mammalian stratum corneum. Our LUV system, which is one of a few model systems using commercially available lipids to include both ceramide types III and IV, simulates the presence of both alpha-hydroxy and non-alpha-hydroxy containing ceramides in the stratum corneum. We also used a combination of commercially available C16 palmitic, C20 lignoceric, and C28 octacosanoic acids to give a mixture of fatty acids with C16 to C28 chain lengths, to closely simulate the free fatty acid composition in the stratum corneum (Wertz et al., 1987). Thus, we believe that the combination of the lipids that we used represent a lipid composition very similar to that in stratum corneum. Our data showed that our LUVs had a relatively uniform size distribution of about 100 - 120 nm at pH 9 in borate buffer with an osmolality of about 150 mmol/kg.

They were stable at room temperature for at least 4 - 6 weeks. Our DSC data were in good agreement with published results on lipids extracted from the stratum corneum, indicating that the lipids in our LUV system were thermodynamically very similar to lipids in intact stratum corneum. Thus, the advantages of our model system are that (1) lipids are easily available, (2) lipids resemble those in the stratum corneum, both in composition and in thermodynamic properties, and (3) it is a stable system with well characterized properties, and thus is well suited for studies of stratum corneum lipid properties under different experimental conditions.

Many phospholipid liposomes have been used as artificial drug carriers (Lasic, 1992). The requirements for clinical application include: (1) a very narrow size distribution and (2) long-term stability (Winterhalter and Lasic, 1993). Our LUV system satisfies both of these requirements, and thus may be suited for further development as carriers for drug or cosmetic delivery.

## 4.2 pH Effects on SC LUVs

Since the surface pH of the skin is about pH 5.5 (Behrendt and Green, 1971; Braun-Falco and Korting, 1986), model systems that can be used at different pH values will be useful. Many of the MLV, SUV or lipid dispersion model systems were prepared at neutral or acidic pH (Friberg and Osborne, 1985; Wertz et al., 1986; Kittayanond et al., 1992; Blume et al., 1993; Kim et al., 1993a; Kitagawa et al., 1993; Mattai et al., 1993). However, these systems cannot be characterized as well as LUV systems for quantitative studies. LUVs with cholesterol sulfate and fatty acids in compositions similar to those found in stratum corneum were all prepared at pH 8.5 or above (Abraham, 1992; Downing et al., 1993), and are

reportedly stable for several weeks. Cholesterol sulfate and/or free fatty acids are needed for lipid systems containing ceramides and cholesterol to form vesicles (Wertz et al., 1986; Kittayanond et al., 1992). The effective $pK_a$ of cholesterol sulfate in membranes is below 4 (Bleau et al., 1974; Kitson et al., 1992). The apparent $pK_a$ of fatty acid in membranes is about 7.2 - 7.4 (Ptak et al., 1980). Thus, cholesterol sulfate and free fatty acids are completely ionized at pH 9. It appears that these charged forms of cholesterol sulfate and fatty acids are required to form stable vesicles with the lipid composition that we used. In these non-phospholipid, stratum corneum lipid vesicle systems, the precise lipid composition and the pH of the aqueous environment appear to be critical to the type of vesicle formed and its stability. In fact, recent $^2H$ NMR studies report that lipid compositions and pH affect the phase behavior of dispersions containing ceramide and palmitic acid, and in combination with cholesterol, phase coexistence is common over the temperature range 20 - 75 °C (Kitson et al., 1994).

As the external pH of the LUVs at pH 9 was lowered to 7.4 and to 6.0 through dialysis, we observed small, gradual increases in effective diameter and polydispersity, and these increases continued as the measurements continued as a function of time leading to unstable vesicles. Since the osmolality of the buffers at different pH values was the same, the observed changes were attributed to pH changes in the samples. It has been noted that borate does not readily permeate vesicle bilayers (Hope and Cullis, 1987). A pH gradient across the bilayer is maintained resulting in lipid asymmetry in vesicles containing phosphatidylcholine and fatty acids prepared at pH 10 and then dialyzed to pH 7 (Wilschut et al., 1992). It is also possible that, in our non-phospholipid LUV system prepared at pH 9 and dialyzed to pH 7.4

or 6.0, a pH gradient was also established between the internal and external aqueous phases with some of the fatty acids moving preferentially toward the inner leaflet of the lipid bilayer where they can maintain their negative charge. Consequently, cholesterol sulfate, at relatively small percentage, was present in the vesicles as the only other negatively charged group in the outer leaflet of the bilayer, rendering relatively unstable vesicles. At pH 6, the LUVs became even less stable because the pH was now approaching values below the $pK_a$ of fatty acids in a membrane. In egg yolk phospholipid vesicles, 5-DSA EPR data indicated the co-existence of both ionized and unionized forms of 5-DSA at pH 6.2 (Egret-Charlier et al., 1978). Interestingly, the effective diameter of our LUVs at pH 6 increased by only about 20 percent before precipitation was observed after 15 h. Since the LUV systems at pH < 9 remained stable for a short period of time, it may be possible to prepare and store LUVs at pH 9, and later to dialyze the samples to low pH values for molecular studies at pH < 9. When this is done, QELS data should accompany the molecular studies to insure the integrity of the LUVs for quantitative interpretation of the data. For example, our QELS data showed that the LUVs at pH 6 were broadly distributed around 128 nm and remained stable for more than 15 but less than 24 h.

## 4.3 Dynamic Properties of Lipids in LUVs

Fatty acid spin labels were used to monitor local dynamic properties of the lipid molecules in the bilayer. 5-DSA reports on motion near the polar headgroup region while 12-DSA describes motion in the center of the alkyl chain (Jost et al., 1971; Smith, 1972; Zhang and Fung, 1994). In phospholipid systems, it is generally accepted that the spin labels are

randomly distributed between the two membrane bilayer leaflets, although the precise distribution is not clear. The nitroxide groups on the stearic acids are located near the lipid molecule head groups, and are closer to the membrane exterior than the analogous position of the phospholipid acyl chains (Ellena et al., 1988). Our results demonstrate that molecular motion near the polar headgroup was more restricted than the motion in the alkyl chain region in the center of the bilayer throughout the temperature range studied (25 - 90 °C). Relatively smaller temperature-induced increases in motion were observed near the polar headgroup region than in the center of the alkyl chain. It is interesting to note that 12-DSA reported rapid changes in motion around 60 °C, a temperature cited as the "melting" of the alkyl chain by infrared and DSC data (Golden et al., 1987). Above 72 °C, little motional change was observed in the alkyl chains upon increase in temperature. The motional properties of lipids in the bilayer depend on molecular packing and molecular interaction among lipid molecules. When an understanding of the distribution of different lipid molecules in the lipid leaflets is available, the local motional properties observed by either 5-DSA or 12-DSA can then be interpreted in more detail.

## 4.4 Partitioning of Fatty Acid Spin Labels in LUVs

Our results showed that the partitioning of fatty acid derivative molecules (spin labels) between lipid and aqueous phases was temperature dependent and generally correlated with the phase transition observed by DSC and the alkyl chain mobility observed by EPR. However, large differences were observed between 5-DSA and 12-DSA molecules. At 25 °C, when 5-DSA was introduced to the LUV system at pH 9 at a lipid-to-label ratio of 150,

almost all 5-DSA was in the lipid phase, and only about 1 % of 5-DSA was in the aqueous phase, with a partition ratio (lipid/aqueous) of 96. However, about 74 % of 12-DSA was in the lipid phase, and about 26 % in the aqueous phase, with a partition ratio of about 3. Partitioning of 5-DSA into the aqueous phase increased upon temperature increase to about 5 % to give a partition ratio of 23 at 90 °C. In contrast, for 12-DSA, relatively small changes in the partitioning of 12-DSA were observed between 25 and 90 °C. Among the small temperature-induced changes for 12-DSA, a minimum partition coefficient at about 40 °C was observed. At this time, no molecular mechanism is obvious for explaining this phenomena. However, the differences observed between the partitioning of 5-DSA and 12-DSA in LUVs at pH 9 can be speculated. 5-DSA and 12-DSA are both derived from stearic acid, with the plane of the doxyl ring perpendicular to the long axis of the molecule (Broldo et al., 1982). Thus the only structural difference between these two molecules is the position of the doxyl spin label moiety, at C5 for 5-DSA and C12 for 12-DSA. This small structural difference produces different polarities for the two molecules. Since van der Waals interactions are important in lipid alkyl chain packing, the location of the doxyl spin label on the alkyl chain is expected to affect the overall polarity and hydrophobicity of the molecules, and thus affect the partitioning of the molecules in the bilayer. The difference in partitioning of 12-DSA and 5-DSA has also been noted for phospholipid vesicles (Sentjurc et al., 1990). It is also interesting to note that the melting point was 51 - 53 °C for 5-DSA and 10 - 12 °C for 12-DSA (Technical information from Aldridge). Our results suggested that in designing drug molecules with somewhat polar functional groups (for example, similar to that of the nitroxide moiety) to be in the stratum corneum lipid phase, it is desirable to attach the

functional group to a fatty acid molecule close to the headgroup position to provide about 99 % partitioning into the lipid phase.

## 4.5 Summary of Development and Molecular Characterization of Model LUV System

In summary, we have used commercially available lipids to successfully prepare relatively stable and well characterized LUVs with lipid compositions and thermodynamic properties very similar to those in stratum corneum. We also demonstrated the time-dependent pH effects on the size and dispersity of the LUVs. Spin label EPR results indicated more restricted motion near the polar region than near the alkyl chain region. We also showed that the partitioning of 5-DSA and 12-DSA between LUV lipid and aqueous phases under similar conditions were quite different from each other. We believe that these results provide foundations for additional studies of stratum corneum LUVs with other molecules and/or of LUVs with different lipid composition leading to better understanding of the physical and functional properties of stratum corneum lipids.

## 4.6 Characterization of Fluorescent Probe Encapsulated SC LUVs

We are interested in lipid interactions between lamellar bilayers of normal SC lipid composition and of abnormal SC lipid composition. Therefore, we have investigated lipid interactions in SC LUVs by vesicle leakage and aqueous contents mixing assays which utilize ANTS/DPX probes (Ellens et al., 1985). Since the lipid composition of the stratum corneum contains only trace amounts of phospholipids (Gray et al., 1982; Wertz et al., 1987), it was necessary to first characterize our non-phospholipid, probe-containing LUVs for lipid

composition, LUV effective diameter and polydispersity, ANTS binding to lipid bilayers and ANTS quenching by DPX in LUVs. In contrast to phospholipid vesicles, we found that LUVs with an effective diameter of about 120 nm in size could not easily be formed with the high concentrations (above 50 mM) of ANTS and DPX probes used in the aqueous contents mixing assay. By preparing several different LUV samples with encapsulated probe concentrations from 12.5 to 90 mM, we found that the optimum concentration to use for the leakage assay was 12.5 mM ANTS and 25 mM DPX. Quenching data for ANTS by DPX in LUVs revealed that these concentrations resulted in ~80 % quenching of ANTS by DPX. For the aqueous contents mixing assay, these values were doubled to 25 mM ANTS and 50 mM DPX since probes are separately encapsulated in different populations of vesicles and mixed in a 1:1 (vol.) ratio.

These concentrations, in general, produced LUVs with effective diameters of about 120 nm for the three different lipid compositions containing different levels of cholesterol and cholesterol sulfate used in our study. The polydispersities of these LUVs were greater than 0.10 but less than 0.16, with higher values near 0.18 obtained for DPX LUVs containing no cholesterol sulfate. These values suggested that a broader distribution of sizes were present than that observed for LUVs prepared without probes. The probe effect was further emphasized by the similar results obtained for LUVs with low (70 mM) and high (130 mM) KCl concentrations present in the aqueous phase. We found that the osmolality increase caused by KCl did not produce a change in the effective diameter or the polydispersity of the LUVs. Instead, it was the difficulty of encapsulating these bulky, charged probes inside the SC LUVs that resulted in a greater distribution of diameters (i.e. polydispersity). In addition,

we found that ANTS did not bind to SC lipid bilayers. Furthermore, in spite of the difficulty of preparing LUVs encapsulated with ANTS and DPX, the lipid composition of the final LUVs was similar to the starting lipid composition. Thus, we suggested that these LUVs were suitable for fluorescence leakage and contents mixing assays.

## 4.7 Comparison of pH 6-Induced Leakage and Contents Mixing with pH 9 Results

Altering the cholesterol sulfate:cholesterol ratio did not affect the leakage and aqueous contents mixing at pH 9. The slight % change in leakage (<1 %) and the small change in aqueous contents mixing (2 - 5 %) suggested that these SC LUVs were relatively stable over the five-hour experimental period. When the SC LUVs containing 5 or 15 % cholesterol sulfate and 25 or 15 % cholesterol, respectively, were lowered to pH 6, gradual increases in leakage and contents mixing were observed over 5 h. The increases were faster over the first 30 min and then gradually increased over the next 4.5 h. LUVs containing 5 % cholesterol sulfate exhibited slightly more leakage and contents mixing than LUVs containing 15 % cholesterol sulfate. This suggests that a lower cholesterol sulfate:cholesterol ratio (i.e. 1:5 instead of 1:1) promotes more lipid interactions in LUVs at pH 6. However, variability between different experimental data with different LUV preparations makes it difficult to determine whether these results are significantly different. Variability within experimental data is probably due to slight differences in LUV diameter and lipid concentration. With phospholipid vesicles, it was found that small changes in the average vesicle size measured by QELS resulted in significant changes in fusion kinetics (Bentz et al., 1985). The destabilization of LUVs at pH 6 versus pH 9 may be due to the neutralization of the fatty acid

carboxylate group at the surface of the vesicles as has been speculated for the fusion of phosphatidylethanolamine/oleic acid vesicles at pH 6. It has been suggested that neutralization of the fatty acid allows the vesicles to closely approach each other (Duzgunes et al., 1985). As discussed earlier in this dissertation, we have observed increases in LUV effective diameter and polydispersity as a function of time in normal lipid composition SC LUVs when the pH is lowered from 9 to 6 by dialysis. This provides further evidence for the pH 6-induced destabilization of SC LUVs.

Contents mixing for SC LUVs with no cholesterol sulfate was similar to results obtained with 5 and 15 % cholesterol sulfate-containing SC LUVs; all compositions resulted in gradual increases in pH 6-induced contents mixing over time. However, in contrast to cholesterol sulfate-containing LUVs, the LUVs without cholesterol sulfate showed quite different leakage profiles. The pH 6-induced leakage of SC LUVs containing no cholesterol sulfate was initially very slow, with a lag phase over the first hour while the leakage of SC LUVs containing cholesterol sulfate did not show a 1 h lag phase . However, after 1 h, leakage of SC LUVs without cholesterol sulfate increased steadily to values significantly greater than those obtained with cholesterol sulfate-containing LUVs. These results suggest that SC LUVs containing cholesterol sulfate slowly leak while fusion is occurring at pH 6. In contrast, SC LUVs without cholesterol sulfate leak after fusion has occurred. This result was similar to the $Ca^{2+}$-induced leakage of ANTS and DPX from PS vesicles (Ellens et al., 1985; Bentz et al., 1985). In this example, fusion was initially non-leaky with massive release of contents occurring after fusion. These authors suggested that the massive vesicle leakage after fusion was probably due to the collapse of fused vesicles into anhydrous cochleate

structures (Wilschut et al., 1980; Ellens et al., 1985).

## 4.8 Comparison of $Ca^{2+}$-Induced Leakage and Contents Mixing at pH 9

$Ca^{2+}$ (5 mM) promoted the fusion of all SC LUVs with different levels of cholesterol and cholesterol sulfate to a greater extent than pH reduction from 9 to 6. In particular, the $Ca^{2+}$-induced aqueous contents mixing profile was similar in all three lipid compositions studied; rapid fusion was observed within the first three min of measurements with little change over 5 h. The leakage profiles, however, were somewhat slower than those observed for contents mixing for all three lipid compositions studied. Leakage was slower than contents mixing with the fastest leakage occurring over the first 30 min. There was no difference between 5 and 15 % cholesterol sulfate-containing LUVs which suggests that the that altering the cholesterol sulfate:cholesterol ratio from 1:5 to 1:1 does not affect $Ca^{2+}$-induced contents mixing or leakage. However, the presence of cholesterol sulfate in the LUVs does effect SC LUV leakage. The LUVs with no cholesterol sulfate initially leaked their contents more slowly than cholesterol sulfate-containing LUVs. After the first 30 min, however, leakage occurred more rapidly and significantly exceeded values obtained for cholesterol sulfate-containing SC LUVs. Therefore, it appears that for SC LUVs without cholesterol sulfate, leakage occurs after fusion, with a massive release of contents after fused structures collapse similar to pH 6 results.

Our results are in agreement with those obtained by Abraham and coworkers (1987) which demonstrated that free fatty acids are necessary for $Ca^{2+}$-induced fusion of vesicles composed of SC lipids. They used EM techniques to show that SUVs composed of

ceramides, cholesterol, and palmitic acid formed lamellar sheets in the presence of $Ca^{2+}$, while SUVs composed of ceramides, cholesterol and cholesterol sulfate did not fuse in the presence of $Ca^{2+}$. In addition, Abraham and coworkers found that SUVs composed of ceramides, cholesterol, palmitic acid and cholesterol sulfate (all present in different percentages than those used by us) exhibited fusion to larger vesicles and some lamellar sheets in the presence of $Ca^{2+}$.

## 4.9 Speculation on the Physiological Significance of Leakage and Fusion of SC LUVs

Our results demonstrated that altering the cholesterol sulfate:cholesterol weight ratio of SC LUVs from 5:1 to 1:1 did not significantly effect the contents mixing and leakage induced by 5 mM $Ca^{2+}$ addition or a decrease in pH from 9 to 6. This suggests that the cholesterol sulfate:cholesterol ratio designated to represent recessive x-linked ichthyosis lipid composition is not by itself enough to prevent SC lipid bilayers from merging and forming larger structures in vitro. However, our results indicated that the presence of cholesterol sulfate in SC lipid bilayers affects the way SC lipid vesicles interact with one another. Whether fusion is induced by low pH or calcium, the leakage of SC LUVs without cholesterol sulfate was, at first, delayed and then massive. These results suggest that the fusion of SC LUVs without cholesterol sulfate is non-leaky and then massive due to vesicle collapse. Thus, the inclusion of cholesterol sulfate in lipid systems for structural and functional studies of the stratum corneum is important. The possible physiological significance of cholesterol sulfate in the stratum corneum, as well as other biological membranes, is commented upon in a recent study by Rodrigueza and coworkers (1995) on the transbilayer movement of

cholesterol and cholesterol sulfate between liposomal membranes. They find that the rate of cholesterol sulfate intermembrane exchange is ten-fold faster than cholesterol with the rapidly exchanging cholesterol sulfate pool located in the outer half of the lipid bilayer. They comment that since the biological role of cholesterol sulfate is unknown, they cannot say whether the large difference in exchange kinetics is functionally important *in vivo*. However, the increased presence of cholesterol sulfate in the epidermis (Williams, 1992), as opposed to the lower layers of the skin, suggests that cholesterol sulfate may play an important role in the structural arrangement of lipids in the stratum corneum. The fact that altering the cholesterol sulfate:cholesterol levels in our LUVs did not prevent the SC LUVs from coming together and mixing their aqueous contents suggests that different lipid component(s) are responsible for the merging of bilayers and mixing of aqueous phases. However, the differences which we observed in both the pH and $Ca^{2+}$-induced leakage of SC LUVs with and without cholesterol sulfate present indicate that the interaction of lipid components in SC lipid bilayers is affected by even small quantities of cholesterol sulfate.

The fusion of lipid vesicles is a complicated process. It would be interesting to study lipid bilayer mixing with the lipid compositions used in this study in order to help elucidate a mechanism for $Ca^{2+}$ or pH-induced fusion. For example, the lipid mixing kinetics of phospholipid vesicles have been compared with contents mixing kinetics in order to increase understanding of the membrane events accompanying fusion (Duzgunes et al., 1987). In addition, it would be interesting to study $Ca^{2+}$-induced fusion at pH 6. Since lowering the pH from 9 to 6 will affect the surface charge of the outer bilayer of LUVs, $Ca^{2+}$-induced leakage and contents mixing might exhibit a completely different profile. In LUVs composed of

dioleoylphosphatidylcholine, dioleoylphosphatidylethanolamine, phosphatidylinositol and dioleoylphosphatidic acid, lipid asymmetry was induced by establishment of a pH gradient, and differences in $Ca^{2+}$-induced fusion were observed (Eastman et al., 1992). Finally, since changing the cholesterol sulfate:cholesterol ratio from 1:1 and 1:5 did not change the fusion profile (measured as aqueous contents mixing and leakage) of LUVs, it would be interesting to further alter the lipid composition of the vesicles to include either all alpha-OH containing ceramides or non-alpha-OH containing ceramides and determine the effect of this structural change on leakage and contents mixing. Since treatment of the skin with alpha hydroxy acids reduces corneocyte cohesion and promotes a thinner SC (Van Scott and Yu, 1984), altering the ceramide composition of the SC LUVs in addition to cholesterol sulfate and cholesterol levels may influence SC vesicle fusion. The importance of stratum corneum ceramide content and composition in the hereditary ichthyoses has recently been investigated (Paige et al., 1994).

## REFERENCES


Abraham, W. *Sem. in Dermatol.* **1992**, *11*, 121-128.

Abraham, W.; Downing, D. *Biochim. Biophys. Acta* **1990**, *1021*, 119-125.

Abraham, W.; Wertz, P. W.; Downing, D. T. *Biochim. Biophys. Acta* **1988a**, *939*, 402-408.

Abraham, W.; Wertz, P. W.; Downing, D. *J. Invest. Dermatol.* **1988b**, *90*, 259-262.

Abraham, W.; Wertz, P. W.; Landmann, L.; Downing, D. T. *J. Invest. Dermatol.* **1987**, *88*, 212-214.

Ahkong, Q. F.; Kitson, N.; Hope, M. J. *J. Invest. Dermatol.* **1992**, *98*, 642a.

Barenholz, Y.; Patzer, E. J.; Moore, N. F.; Wagner, R. R. *Adv. Exp. Med. Biol.* **1978**, *101*, 45-56.

Behrendt, H.; Green, M. *Patterns of skin pH from birth through adolescence*; Charles C. Thomas: Springfield, IL, 1971.

Bentz, J.; Duzgunes, N.; Nir, S. *Biochemistry* **1985**, *24*, 1064-1072.

Blank, I. H. *J. Invest. Dermatol.* **1952**, *18*, 433-440.

Bleau, G.; Bodley, F. H.; Longpre, J.; Chapdelaine, A.; Roberts, K. D. *Biochim. Biophys. Acta* **1974**, *352*, 1-9.

Blume, A.; Jansen, M.; Ghyczy, M.; Gareiss, J. *Inter. J. Pharmaceut.* **1993**, *99*, 219-228.

Braun-Falco, O.; Korting, H. *Hautarzt* **1986**, *37*, 126-129.

Broldo, M. S.; Belsky, I.; Melrovitch, E. *J. Phys. Chem.* **1982**, *86*, 4197-4205.

Brown, L. R.; Bösch, C.; Wüthrich, K. *Biochim. Biophys. Acta* **1981**, *642*, 296-312.

Brysk, M. M.; Rajaraman, S. *Progr. Histochem. Cytochem.* **1992**, *25(1)*, 1-53.

Downing, D. T. *J. Lipid Res.* **1992**, *33*, 301-313.

Downing, D. T.; Abraham, W.; Wegners, B. K.; William, K. M.; Marshall, J. L. *Arch. Dermatol. Res.* **1993**, *285*, 151-157.

Duzgunes, N.; Staubinger, R. M.; Baldwin, P. A.; Friend, D. S.; Papahadjopoulos, D. *Biochemistry* **1985**, *24*, 3091-3098.

Duzgunes, N.; Allen, T. M.; Fedor, J.; Papahadjopoulos, D. *Biochemistry* **1987**, *26*, 8435-8442.

Eastman, S. J.; Hope, M. J.; Wong, K. F.; Cullis, P. *Biochemistry* **1992**, *31*, 4262-4268.

Eastman, S.; Wilschut, J.; Cullis, P. R.; Hope, M. J. *Biochim. Biophys. Acta* **1989**, *981*,178-184.

Egret-Charlier; Sanson, M. A.; Ptak, M. *FEBS Lett.* **1978**, *89*, 313-316.

Elias, P. M.; Williams, M. L.; Maloney, M. E.; Bonifas, J. A.; Brown, B. E.; Grayson, S.; Epstein Jr., E. H. *J. Clin. Invest.* **1984**, *74*, 1414-1421.

Elias, P. M.; Friend, D. *J. Cell. Biol.* **1975**, *65*, 180-191.

Ellena, J.; Archer, S.; Dominey, R.; Hill, B.; Cafiso, D. *Biochim. Biophys. Acta* **1988**, *940*, 63-70.

Ellens, H.; Bentz, J.; Szoka, F. C. *Biochemistry* **1985**, *24*, 3099-3106.

Ellens, H.; Bentz, J.; Szoka, F. C. *Biochemistry* **1984**, *23*, 1532-1538.

Freed, J. H. In *Spin labeling. Theory and Applications*; Berliner, L. J., Ed.; Academic Press; New York, 1976; pp 53-132.

Friberg, S. E.; Osborne, D. W. *J. Dispers. Sci. and Tech.* **1985**, *6*, 485-495.

Fung, L. W.-M.; Johnson, M. E. In *Current Topics in Bioenergetics*; Lee, P., Ed.; Academic Press, New York, 1984; pp 107-157,

Fung, L. W.-M.; Johnson, M. E. *Biophys. J.* **1983**, *43*, 255-257.

Fung, L. W.-M.; Zhang, Y. *Free Rad. Biol. Med.* **1990**, *9*, 289-298.

Golden, G. M.; Guzek, D. B.; Kennedy, A. H.; McKie, J. E.; Potts, R. O. *Biochemistry*

**1987**, *26*, 2382-2388.

Golden, G. M.; Guzek, D. B.; Harris, R. R.; McKie, J. E.; Potts, R. O. *J. Invest. Dermatol.* **1986**, *86*, 255-259.

Gray, G. M.; White, R. J. *Biochem. Soc. Trans. (London)* **1979**, *7*, 1129-1131.

Gray, G. M.; White, R. J.; Williams, R. H.; Yardley, H. J. *Brit. J. Dermatol.* **1982**, *106*, 59-63.

Griffith, O. H.; Dehlinger, P. J.; Van, S. P. *J. Memb. Biol.* **1974**, *15*, 159-192.

Griffith, O.H.; Jost, P. C. In *Spin Labeling. Theory and Applications*; Berliner, L. J., Ed.; Academic Press: New York, 1976; pp 453-523.

Hadgraft, J.; Walters, K. A.; Guy, R. H. *Sem. in Dermatol.* **1992**, *11*, 139-144.

Hope, M. J.; Bally, M. B.; Webb, G.; Cullis, P. R. *Biochim. Biophys. Acta* **1985**, *812*, 55-65.

Hope, M. J.; Cullis, P. R. *J. Biol. Chem.* **1987**, *262*, 4360-4366.

Hou, S. Y. E.; Rehfeld, S. J.; Plachy, W. Z. *Adv. Lipid Res.* **1991**, *24*, 141-171.

Johnson, M. E. *Biochemistry* **1979**, *18*, 378-384.

Jost, P.; Libertini, L. J.; Herbert, V. C.; Griffith, O. H. *J. Mol. Biol.* **1971**, *59*, 77-98.

Kim, C.-K.; Hong, M.-S.; Kim, Y.-B.; Han, S.-K. *Intern. J. Pharmaceut.* **1993a**, *95*, 43-50.

Kim, Y.-H.; Higuchi, W. I.; Herron, J. N.; Abraham, W. *Biochim. Biophys. Acta* **1993b**, *1148*, 139-151.

Kitagawa, S.; Sawada, M.; Hirata, H. *Intern. J. Pharmaceut.* **1993**, *98*, 203-208.

Kitson, N.; Monek, M.; Wong, K.; Thewalt, J.; Cullis, P. *Biochim. Biophys. Acta* **1992**, *1111*, 127-133.

Kitson, N.; Thewalt, J.; Lafleur, M.; Bloom, M. *Biochemistry* **1994**, *33*, 6707-6715.

Kittayanond, D.; Ramachandran, C.; Weiner, N. *J. Soc. Cosmet. Chem.* **1992**, *43*, 149-160.

Klösgen, B.; Helfrich, W. *Eur. Biophys. J.* **1993**, *22*, 329-340.

Lampe, M. A.; Burlingame, A. L.; Whitney, J.; Williams, M. L.; Brown, B. E.; Roitman, E.; Elias, P. M. *J. Lipid Res.* **1983**, *24*, 120-130.

Lasic, D. D.Liposomes. *Am. Sci.* **1992**, *80*, 20-31.

Madison, K. C.; Swartzendruber, D. C.; Wertz, P. W; Downing, D. T. *J. Invest. Dermatol.* **1987**, *88*, 714-718.

Marsh, D. *Techniques in Life Sciences (Lipid and Membrane Biochemistry-Part II)*. **1982**, *B4/II, B426*, 1-44.

Mattai, J.; Froebe, C. L.; Rhein, L. D.; Simion, F. A.; Ohlmeyer, H.; Su, D. T.; Friberg, S. E. *J. Soc. Cosmet. Chem.* **1993**, *44*, 89-100.

Mayer, L. D.; Hope, M. J.; Cullis, P. R.; Janoff, A. S. *Biochim. Biophys. Acta* **1985**, *817*, 193-196.

Melnik, B. C.; Hollmann, J.; Erler, E.; Verhoeven, B.; Plewig, G. *J. Invest. Dermatol.* **1989**, *92*, 231-234.

Miyazaki, J.; Kalman, H.; Marsh, D. *Biochim. Biophys. Acta* **1992**, *1108*, 62-68.

Onken, H. D.; Moyer, C. A. *Arch. Dermatol.* **1963**, *87*, 584-590.

Paige, D. G.; Morse-Fisher, N.; Harper, J. I. *Br. J. Dermatol.* **1994**, *131*, 23-27.

Ptak, M.; Egret-Charlier, M.; Sanson, A.; Bouloussa, O. *Biochim. Biophys. Acta* **1980**, *600*, 387-397.

Rodrigueza, W. V.; Wheeler, J. J.; Klimuk, S. K.; Kitson, C. N.; Hope, M. J. *Biochemistry* **1995**, *34*, 6208-6217.

Scheuplein, R. J.; Blank, I. H. *Physiol. Rev.* **1971**, *51*, 702-747.

Sentjurc, M.; Bacic, G.; Swartz, H. M. *Arch. Biochem. Biophys.* **1990**, *282*, 207-213.

Sharpiro, L. J.; Weiss, R.; Webster, D.; France, J. T. *Lancet* **1978**, *1*, 70-72.

Smith, I. C. P. In *Biological applications of electron spin resonance*; Swartz, H. M., Bolton, J. R. & Borg, D. C., Eds.; Wiley Interscience: New York, 1972; pp 483-539.

Smolarsky, M.; Teitelbaum, D.; Sela, M.; Gitler, C. *J. Immunol. Methods* **1977**, *15*, 255-265.

Struck, D. K.; Hoekstra, D.; Pagano, R. E. *Biochemistry* **1981**, *20*, 4093-4099.

Szoka, F. C. In *Cell Fusion* ; Sowers, A. E., Ed.; Plenum Press: New York, 1987; pp 209-240.

Van Scott, E. J.; Yu, R. J. *J. Am. Acad. Dermatol.* **1984**, *11*, 867-879.

Weinstein, J. N.; Yoshikami, S.; Henkart, P.; Blumenthal, R.; Hagins, W. A. *Science* **1977**, *195*, 489-503.

Wertz, P. W.; Swartzendruber, D. C.; Madison, K. C.; Downing, D. T. *J. Invest. Dermatol.* **1987**, *89*, 419-425.

Wertz, P. W.; Abraham, W.; Landmann, L.; Downing, D. T. *J. Invest. Dermatol.* **1986**, *87*, 582-584.

White, S. H.; Mirejovsky, D.; King, G. I. *Biochemistry* **1988**, *27*, 3725-3732.

Williams, A. C.; Barry, B. W. *Crit. Rev. Therapeut. Drug Carrier Sys.* **1992**, *9*, 305-353.

Williams, M. L. *Sem. in Dermatol.* **1992**, *11*, 169-175.

Williams, M. L.; Elias, P. M. *J. Clin. Invest.* **1981**, *68*, 1404-1410.

Wilschut, J.; Scholma, J.; Eastman, S. J.; Hope, M. J.; Cullis, P. R. *Biochemistry* **1992**, *31*, 2629-2636.

Wilschut, J.; Duzgunes, N.; Fraley, R.; Papahadlopoulos, D. *Biochemistry* **1980**, *20*, 3126-3133.

Winterhalter, M.; Lasic, D. D. *Chem. Phys. Lipids* **1993**, *64*, 35-43.

Zhang, Y.; Fung, L. W.-M. *Free Rad. Biol. Med.* **1994**, *16*, 215-222.

# VITA

The author, Rita Mrowca Hatfield, was born on March 4, 1966 in Chicago, Illinois. In August 1984, she entered the University of Notre Dame in South Bend, Indiana and received a Bachelor of Science degree with honors in May, 1988. During her last two and one half years at Notre Dame, Ms. Hatfield was involved in undergraduate research in Biochemistry. She also was fortunate to work in several different types of research environments during the summers of her undergraduate years including Argonne National Laboratory, the Department of Pharmacology at the University of Illinois at Chicago, and Stepan Chemical Company (Northfield, IL).

Ms. Hatfield worked for Helene Curtis Ind., Inc. (Chicago, IL) as a Research and Development Scientist II from February 1989 to April 1991 in the Claims Substantiation/Biophysical Testing Group. She was promoted to Scientist I in April 1991 and worked in this capacity until August 1992. Ms. Hatfield began part time graduate work in the Chemistry Department of Loyola University of Chicago in January 1991 and became a full time student on paid leave from Helene Curtis in August of 1992 to perform research under the direction of Professor Leslie W.-M. Fung. Ms. Hatfield has been supported by Helene Curtis Industries during her tenure at Loyola as part of a collaborative research project between the company and Loyola to study biophysical properties of the stratum corneum on the molecular level.

Ms. Hatfield served the Chemistry Department at Loyola University of Chicago as the Student Faculty Representative of the Chemistry Graduate Student Organization in the 1992/93 academic year. She participated and won first prize for a Poster Presentation at the Sigma Xi 24th Annual Graduate Student Forum of Loyola University in May, 1994. Ms. Hatfield also presented a poster at the Gordon Research Conference on the Barrier Properties of Mammalian Skin (Plymouth, New Hampshire) in August, 1993 and was awarded a Young Investigator's Scholarship by the conference organizers to attend the conference. As a participating member of the Biophysical Society, Ms. Hatfield has presented her research in poster form at the annual 1994 and 1995 meetings in New Orleans, Louisiana and San Francisco, California, respectively. The author's formal publications from graduate work include "Molecular Properties of a Stratum Corneum Model Lipid System: Large Unilamellar Vesicles" by Rita M. Hatfield and Leslie W.-M. Fung (1995) Biophysical Journal 68, 196-207.

Ms. Hatfield was married in October, 1992, shortly after beginning full time graduate studies at Loyola. She and her husband are expecting their first child in February.

DISSERTATION APPROVAL SHEET

The dissertation submitted by Rita M. Hatfield has been read and approved by the following committee:

Leslie W.-M. Fung, Ph.D., Director
Professor, Chemistry
Loyola University Chicago

Daniel J. Graham, Ph.D.
Associate Professor, Chemistry
Loyola University Chicago

Robert Harper, Ph.D.
Director of Product Safety
Hilltop Research, Cincinnati, OH

Patrick M. Henry, Ph.D.
Professor, Chemistry
Loyola University Chicago

Priscilla L. Walling, Ph.D.
Senior Manager, Technology Development
Helene Curtis Industries, Inc., Rolling Meadows, IL.

The final copies have been examined by the director of the dissertation and the signature which appears below verifies the fact that any necessary changes have been incorporated and that the dissertation is now given final approval by the committee with reference to content and form.

The dissertation is, therefore, accepted in partial fulfillment of the requirements for the degree of Doctor of Philosophy.

Dec. 1, 1995.
Date

Director's Signature